horticulturae

MDPI

Review

Top Ten Most Important U.S.-Regulated and Emerging Plant-Parasitic Nematodes

Mihail Kantor [1], Zafar Handoo [1,*], Camelia Kantor [2] and Lynn Carta [1]

[1] Mycology and Nematology Genetic Diversity and Biology Laboratory, USDA, ARS, Northeast Area, Beltsville, MD 20705, USA; mihail.kantor@usda.gov (M.K.); lynn.carta@usda.gov (L.C.)
[2] Huck Institutes of the Life Sciences, Pennsylvania State University, State College, PA 16802, USA; cmk6719@psu.edu
* Correspondence: zafar.handoo@usda.gov

Abstract: Plant-parasitic nematodes (PPNs) are important pests that cause an estimated ten billion dollars of crop loss each year in the United States and over 100 billion dollars globally. The Animal and Plant Health Inspection Service (APHIS) within the U.S. Department of Agriculture maintains and updates the U.S. Regulated Plant Pest list. Currently, the number of PPNs regulated by APHIS includes more than 60 different species. This review focuses on the top ten most economically important regulated and emerging plant-parasitic nematodes and summarizes the diagnostics of morphological and some molecular features for distinguishing them. These ten major previously described nematode species are associated with various economically important crops from around the world. This review also includes their current distribution in the U.S. and a brief historical background and updated systematic position of these species. The species included in this review include three PPNs considered by the U.S. Department of Agriculture as invasive invertebrates *Globodera pallida*, *Globodera rostochiensis*, and *Heterodera glycines*; four regulated PPNs, namely *Bursaphelenchus xylophilus*, *Meloidogyne fallax*, *Ditylenchus dipsaci*, and *Pratylenchus fallax;* and the three emerging PPNs *Meloidogyne chitwoodi*, *Meloidogyne enterolobii*, and *Litylenchus crenatae mccannii*.

Keywords: APHIS; *Bursaphelenchus xylophilus*; *Ditylenchus dipsaci*; *Globodera pallida*; *Globodera rostochiensis*; *Litylenchus crenatae mccannii*; *Meloidogyne chitwoodi*; *Meloidogyne enterolobii*; *Meloidogyne fallax*; *Pratylenchus fallax*; regulated and emerging plant-parasitic nematodes

Citation: Kantor, M.; Handoo, Z.; Kantor, C.; Carta, L. Top Ten Most Important U.S.-Regulated and Emerging Plant-Parasitic Nematodes. *Horticulturae* **2022**, *8*, 208. https://doi.org/10.3390/horticulturae8030208

Academic Editor: Carlos Gutiérrez Gutiérrez

Received: 31 January 2022
Accepted: 21 February 2022
Published: 26 February 2022

1. Introduction

In the United States, the Department of Agriculture regulates and oversees pests and diseases, especially through the Animal and Plant Health Inspection Service (APHIS) agency. APHIS protects the United States' agricultural interests as well as monitors existing agricultural pests and diseases. APHIS maintains and regularly updates the U.S. Regulated Plant Pest [1]. The table with Regulated Plant Pests provided by APHIS includes a list of more than 60 PPN species [1].

The National Invasive Species Information Center (NISIC) was established in 2005 at the USDA's National Agricultural Library (NAL) to meet the information needs of users [2]. NISIC included in their list of terrestrial invertebrates three PPN species, namely *Globodera pallida*, *Globodera rostochiensis* and *Heretodera glycines* [2]. *G. pallida* and *G. rostochiensis* are perhaps the most important species of PPNs and are subject to strict regulatory restrictions in the United States and other countries [3]

Globally, PPNs are considered important pests and are responsible for important crop losses, with an estimated annual loss of USD 173 billion [4]. Potato cyst nematodes (PCN) have a global distribution and economic impact on potato crops [5,6]. Together, *Globodera pallida* and *G. rostochiensis* are responsible for potato crop losses of approximately 9% worldwide [7,8].

Heterodera glycines or soybean cyst nematode (SCN) is another plant-parasitic nematode listed under the NISIC list. The SCN continues to be the most devastating pest of soybean throughout U.S. and Canadian soybean-producing areas [9]. A recent census conducted in 2020 by Tylka and Marett [9] revealed a steady expansion of the distribution of SCN throughout the U.S. and Canada. The SCN was first reported in the U.S. in 1954 from North Carolina, almost 40 years after it was first identified in Japan in 1915 [10].

Bursaphelenchus xylophilus, or the pine wood nematode, is included in the APHIS U.S. Regulated Plant Pest Table [1] and is the causal agent of pine wilt disease. The pine wood nematode is native to North America and is one of the most damaging pest problems to forests around the world [11]. Many countries outside of the U.S. have labeled *Bursaphelenchus xylophilus* as a quarantine nematode because of its potential for destruction of their native conifers [11].

Meloidgyne fallax, or false Columbia root-knot nematode, is another nematode included in the APHIS U.S. Regulated Plant Pest Table [1]. It has a wide host range, which includes several major horticultural and agricultural crops. In potato, this nematode could lead to total yield losses due to quality defects caused to the tubers [12,13]. In the U.S., the false Columbia root-knot nematode was first reported in 2013 from a golf course in San Francisco, California [14]. After conducting a nematode survey in golf courses from several counties in California, APHIS did not find this nematode, listing this species as not present in the U.S. [15].

Meloidogyne chitwoodi is another root-knot nematode species considered as an important pathogen of economically important crops, especially potatoes. It is not listed in the APHIS U.S. Regulated Plant Pest Table, but it is on the lists of prohibited organisms in many other countries such as Canada, Mexico, the EU and in several countries from South America and Asia [13]. In the Pacific Northwest of the U.S, this species is considered as one of the major pests of potatoes [16].

Meloidogyne enterolobii, or the guava root-knot nematode, is a species with many host plants, including cultivated crops and weeds, that can cause significant damage [13,17]. In the U.S., this species was first reported from Florida in 2004 [18]. Currently, this species is not under any in force quarantine requirements. This root-knot nematode species is considered by many nematologists as an emerging pest and should be regulated to prevent its spread.

Litylenchus crenatae mccannii is a newly recognized nematode subspecies that causes beech leaf disease (BLD) in *Fagus grandifolia* [19]. This species is considered an important foliar pathogen that parasitizes beech trees in U.S. [20]. Since the first report of BLD in 2012 from Ohio, the disease has spread across the Northeastern U.S. and has been reported from nine different states [21].

Pratylenchus fallax is a nematode species that is also included in the APHIS U.S. Regulated Plant Pest Table [1]. In the U.S., it was first reported in 1980 [22]. More recently, this nematode was reported on soybean from Wisconsin, thus providing its first molecular characterization in the U.S. [23]. It was also reported in 1997 on turfgrass in Canada (Ontario) [24].

Ditylenchus dipsaci, or the stem and bulb nematode, has a worldwide distribution and is considered a quarantine pest by many countries around the world. This species is also listed in the APHIS U.S. Regulated Plant Pest Table [1], and it has a wide host range, which includes more than 1200 species of cultivated and wild plants [25]. It has a wide U.S. distribution and has been reported from more than 20 different states (CABI-ISC, 2021) [26].

1.1. Bursaphelenchus xylophilus (Steiner & Buhrer, 1934) Nickle, 1970

- *Common name*: pine-wood nematode
- *Type plant host*: *Pinus palustris* Mill. or longleaf Louisiana pine
- *Type locality*: Bogalusa, LA, USA

Measurements: (see Table 1).

Table 1. *Bursaphelenchus xylophilus* morphometrics of females and males (after Nickle et al. [27] courtesy of Marcel Decker Inc.).

Character	Females	Male	Female Allolectotype	Male Hololectotype
	n = 5	n = 5	n = 1	n = 1
L	523.0 (447.0–609.0)	560.0 (520.0–601.0)	544.0	557.0
a	42.6 (37.0–48.0)	40.8 (35.0–45.0)	37.0	38.0
b	9.6 (8.3–10.5)	9.4 (8.4–10.5)	9.0	8.5
c	27.2 (23.0–31.0)	24.4 (21.0–29.0)	28.0	23.0
V%	74.7 (72.7–77.5)	-	73.0	-
Stylet length	12.8 (12.6–13.0)	13.3 (12.6–13.8)	12.6	13.8
Spicule length	-	21.2 (18.8–23.0)	-	21.1
Gubernaculum	-	-	-	-

Description (modified after Nickle et al. [27]).

Female: Lip region offset with six lips. Stylet knobs small. Esophageal glands 3–4 body widths long, overlapping dorsally. Excretory pore most commonly found at opposite junction of esophagus and intestine but sometimes can be found at the level of the nerve ring. Hemizonid prominent, about two-thirds of the body diameter behind the median bulb. Ovary outstretched, oocytes usually in single file. Post uterine sac long, extending three-fourths of the distance to anus. Tail subcylindrical, ending usually with a broad rounded tail terminus.

Male: Spicules large, uniquely arcuate, paired, with sharply pointed prominent rostrum; distal ends of spicules with typical disc-like expansions. Tail arcuate, terminus pointed, appearing talon-like in lateral view, surrounded by short, oval caudal alae. Seven caudal papillae, one adanal pair just pre-anal, single papilla just pre-anal centered; two post-anal pairs just before caudal alae origin.

U.S. Distribution (see Figure 1).

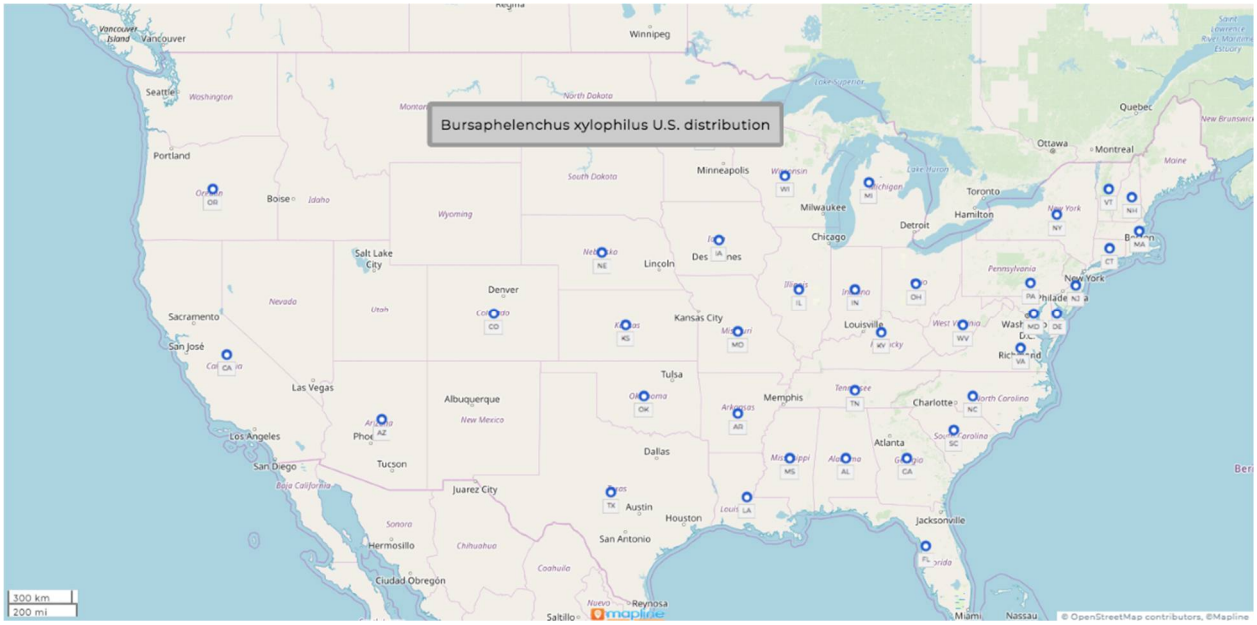

Figure 1. Distribution map of *Bursaphelenchus xylophilus* (adapted from CABI-ISC [26]).

Symptoms: Destruction of cortical and cambial tissues are the most common symptoms associated with this nematode. It is followed by cavitation-induced embolism of xylem tracheids. According to Donald et al. [28], the nematode induces a cascading series of hypersensitive reactions in xylem parenchyma cells as it spreads throughout a susceptible

tree. This can lead to a leakage of cell contents into tracheids and then by disruption of water conduction and tree death [28].

Pathogenicity: *Bursaphelenchus xylophilus* causing pine wilt has an even more significant impact in countries such as China, Japan, Korea, and Taiwan. About 28% of Japan's total pine forest area may be infected with *B. xylophilus*, despite significant dollar amounts (millions) being allocated annually for mitigation and control. Outside of Asia, countries such as Portugal and Spain have also spent millions on control measures of *B. xylophilus* [28]. Some isolates of this species exhibit different host specificity and virulence. For example, isolates from balsam fir and Scot's pine are pathogenic on their original host but not on the other conifer species [28].

Molecular characterization: This species was characterized using the DNA sequences on (1) the ribosomal DNA small subunit, (2) the large subunit D2/D3, (3) the internal transcribed spacer (ITS), and (4) the mitochondrial DNA cytochrome oxidase subunit. Ye and Giblin-Davis [11] sequenced 45 populations of PWN and described the development of a real-time-PCR method for rapid and accurate identification of PWN targeting the ITS-1. In 2019, Kikuchi et al. [29] developed a precise and rapid detection of PWN by loop-mediated isothermal amplification (LAMP).

Diagnosis: This species can be differentiated from others in the genus by the shape of the spicules, the distinct vulva flap, and the absence of a digitate tail tip [26].

1.2. Ditylenchus dipsaci (Kuhn, 1857) Filipjev, 1936

- *Common name*: Stem and bulb nematode
- *Type plant host*: *Dipsacus fullonum* L., fuller's teasel
- *Type locality*: Poppelsdorf near Bonn, Germany
- *First U.S. report*: 1914, Edgerton, KS

Measurements: (see Table 2).

Table 2. *Ditylenchus dipsaci* morphometric of females and males.

	After Thorne [30]		After Blake in Hooper [31]		After Mollov et al. [32]		After Testen et al. [33]	
Character	**Female**	**Male**	**Female**	**Male**	**Female**	**Male**	**Female**	**Male**
			n = 48	n = 23	n = 6	n = 9	n = 16	n = 6
L	1000.0–1300.0	1300.0	1300.0	1000.0–1300.0	1411.0–1636.0	1372.0–1558.0	1080.1 (972.2–1229.5)	1589.2 (1494–1702.7)
a	36.0–40.0	63.0	62.0	37.0–41.0	38.0–44.0	40.0–50.0	36.6 (33.5–41.9)	43.0 (40.7–46.0)
b	6.5–7.1	15.0	15.0	6.5–7.3	5.8–8.0	6.5–7.0	6.2 (5.3–6.8)	6.9 (6.4–7.3)
c	14.0–18.0	14.0	14.0	12.0–15.0	14.0–17.0	14.0–16.0	11.1 (9.1–12.8)	11.7 (9.2–13)
V%	80	-	80	-	79.0–81.0	-	-	-
Stylet length	-	-	-	-	11.5–12.3	11.5–12.3	10.1 (8.9–11.2)	10.8 (10.0–12.2)
Tail length	-	-	-	-	95.0–105.0	-	-	-
Spicule length	-	-	-	-	-	22.0–27.0	-	25.2 (23.0–26.8)
T	-	72.0	-	65.0–72.0	-	-	-	-
Gubernaculum	-	-	-	-	-	9.0–10.0	-	-

Description (modified after Sturhan and Brzeski [34], and Thorne [30]).

Female: Body straight or almost when relaxed, marked by transverse striae, about 1 µm apart. Four lines in the lateral field. Head smooth, continuous with adjacent body. Deirids usually visible near the base of neck. Hemizonid adjacent to excretory pore and about six annules wide. Excretory pore opposite posterior part of isthmus or glandular bulb. Stylet cone about half of stylet length, with strongly developed rounded knobs. Median esophageal bulb muscular, with thickenings of lumen walls about 4–5 um long. Basal bulb offset or overlapping intestine for a few micrometers with three prominent and two inconspicuous gland nuclei. Ovary outstretched, sometimes reaching the median esophageal bulb, most of the times near the basal bulb, rarely with one or two flexures. A rudimentary posterior uterine branch present. Post-vulval part of uterine sac about half of the vulva–anus distance long or slightly more. Tail terminus always acute.

Male: Anterior region same as female. Testis outstretched, with spermatocytes arranged in single file except for a short region of multiplication. Bursa begins opposite the anterior end of the spicule and extends about three-fourths of the length of the tail. Tail always pointed.

U.S. Distribution (see Figure 2).

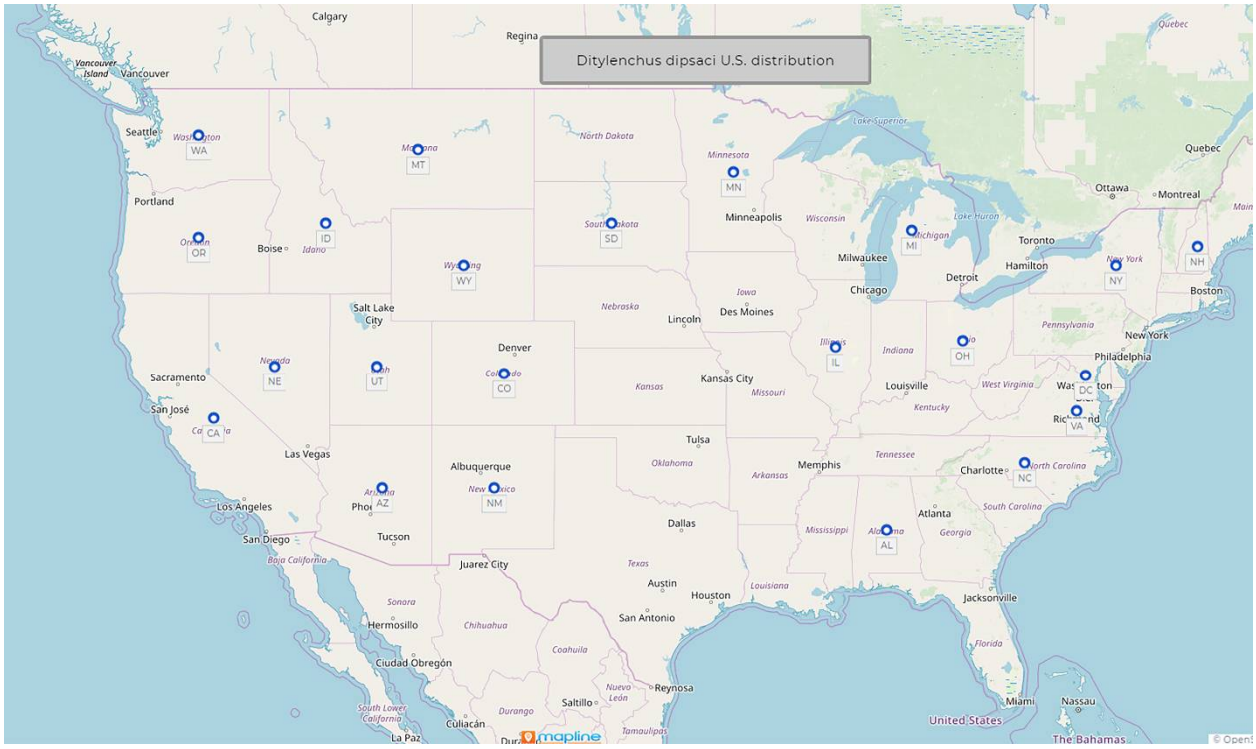

Figure 2. Distribution map of *Ditylenchus dipsaci* (adapted from CABI-ISC) [26].

Symptoms: Damage symptoms caused by this nematode change with host. Most common symptoms include stunting, crinkling, twisting, swelling, or malformation of the leaves, leaf stalks, flowers, and stems. Infested tissue may also split [34].

Pathogenicity: Discovery of this species in bulbs imported from the Netherlands prompted the first regulatory measures against nematodes by the U.S. [30]. *Ditylenchus dipsaci* is one of the most devastating plant-parasitic nematodes on many crops. If high infestations occur, they could lead to crop losses of up to 60–80%. For example, in Italy, up to 60% of onion seedlings died before transplanting, while France and Poland experienced garlic crop losses of more than 90% [35].

Molecular characterization: This species was characterized using the DNA sequences of the D2-D3 expansion segments of the 18 S and 28 S rRNA genes and of the ITS-rRNA region by Mollov et al. [32] and Testen et al. [33]. Subbotin et al. [36] developed species-specific primers for which they used 30 *Ditylenchus dipsaci* populations in a molecular study based on the sequences of the ITS-rRNA region.

Diagnosis: According to Andrássy [37], the number of lateral lines, the stylet and postvulval sac length, and the shape of the tail (pointed) differentiate this species from the others in the genus. As compared to *D. gigas*, this species has a shorter body for females (1.0–1.7 vs. 1.6–2.2 mm) and a longer vulva–anus distance (202–266 vs. 132–188 µm) [38]. The males of this species can be differentiated from *D. destructor* by having a more arched spicule [39].

1.3. Globodera pallida (Stone, 1973) Behrens, 1975

- *Common name*: Pale (white) potato cyst nematode
- *Type plant host*: *Solanum tuberosum* L.

- *Type locality*: Epworth, Lincolnshire, Eastern England
- *First U.S. report*: 2006, ID

Measurements: The morphometric measurements are given in Table 3 after Skantar et al. [40].

Table 3. Morphometrics of diagnostic characters of second-stage juveniles and cysts of *Globodera pallida* from Idaho after Skantar et al. [40] (courtesy of Journal of Nematology).

	G. pallida **Second Stage Juveniles (n = 80)**			***G. pallida*** **Cysts (n = 80)**		
Character	**Range**	**Mean**	**SD**	**Range**	**Mean**	**SD**
Body length	380–533	452.0	36.0	-	-	-
Stylet length	22.5–25.0	23.2	0.7	-	-	-
Tail length	40.0–57.0	49.6	3.0	-	-	-
Hyaline tail terminal length	20.0–31.0	25.9	2.4	-	-	-
Body length excluding neck [a]	-	-	-	420–700	574	85
Body width [b]	-	-	-	400–600	534	80
Distance from anus to nearest edge of fenestra (anus-vulva)	-	-	-	30.0–80.0	53.5	11.8
Fenestra length	-	-	-	17.5–45.0	24.8	5.6
Number of cuticular ridges between vulva and anus	-	-	-	7.0–17.0	12.0	2.5
Granek's ratio	-	-	-	1.2–3.6	2.2	0.5

[a] Based upon measurements of 15 cysts. [b] As modified by Hesling, 1973.

Description (modified after Skantar et al. [40]).

- *Cyst*: The morphological characters of cysts of this population agree with those of *G. pallida* except for the slightly higher mean in the distance from the anus to the nearest edge of fenestra 53.5 (30–80 µm). Both cyst, and J2 morphometrics and J2 tail morphology of the Idaho specimens fit well within the ranges observed for *G. pallida*, indicating that the Idaho specimens must represent *G. pallida*.
- *Juvenile*: The second-stage juveniles morphological characters of the Idaho population are similar to those of *G. pallida* but have a slightly shorter mean body length (452 ± 36 µm) than the lengths reported by Stone (1972) for the Epworth, Lincolnshire, England, population (486 ± 23 µm) and for the Duddingston, Scotland, population (482 ± 18 µm).

U.S. Distribution

Fortunately, since first reported in the U.S. [40], *G. pallida*'s spread has been strictly monitored and limited to only two counties in Idaho (Figure 3).

All the fields from where PCN were identified are regulated and are under strict surveillance and treatment [7]. Currently, there are 7354 acres included in the PCN Eradication Program in Idaho [7]. Regulatory officers collected more than 89,000 soil samples in support of USDA's post-regulation monitoring of fields deregulated by APHIS.

APHIS published a pie chart (Figure 4) that illustrates the PCN eradication progress summary as of 30 June 2021. The pie chart presents the progress for the 31 infested fields detected in Idaho since the first interception in 2006.

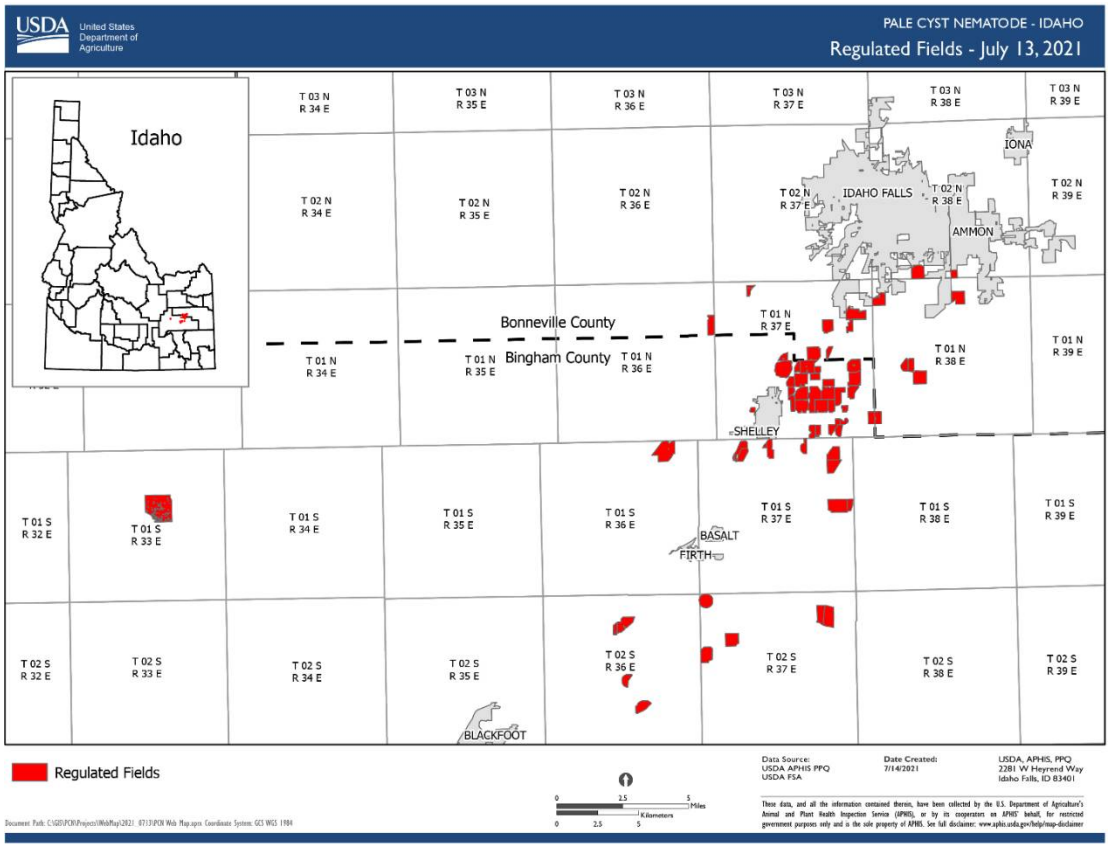

Figure 3. Distribution of *Globodera pallida* in the U.S. (source, USDA, APHIS).

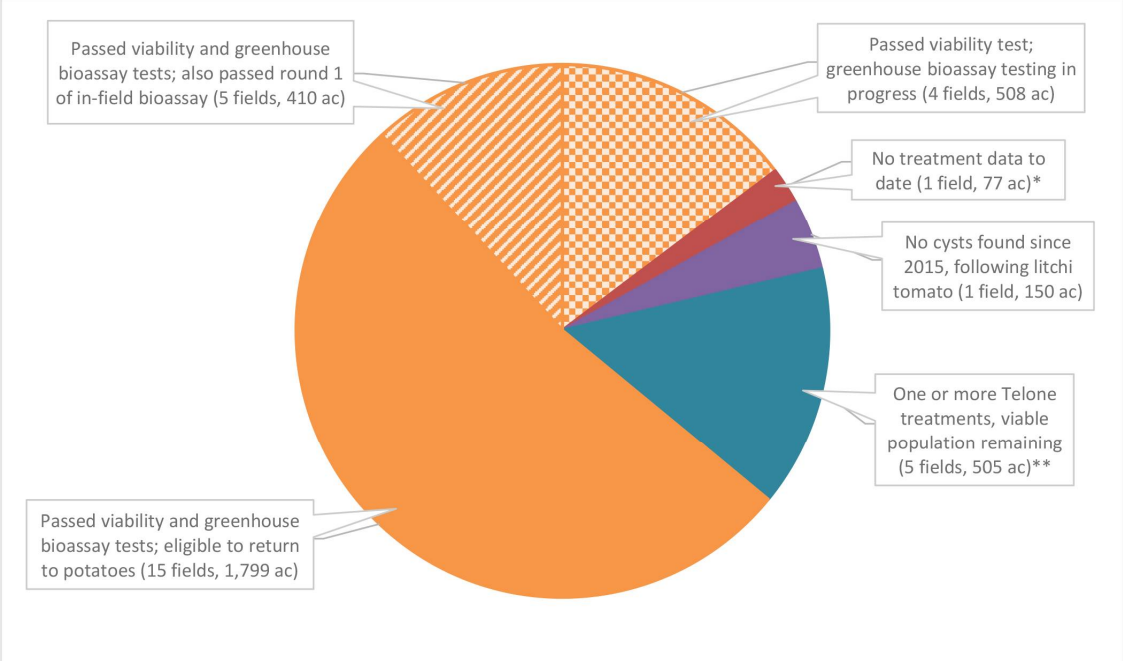

Figure 4. Progress for the 31 infested fields with *Globodera pallida* from Idaho (source, USDA, APHIS). * Field planted with a multi-year alfalfa crop in 2020; ** 2020 data; 2021 post-Telone data will be available by March 2022. This pie slice includes three fields that returned to potato production as part of the in-field bioassay test but viable nematodes were found in post-harvest surveys.

Molecular characterization: PCR-RFLP of the rDNA ITS region, sequence-specific multiplex PCR, and DNA sequences of the Idaho was provided by Skantar et al. [40]. A detailed molecular study conducted by Subbotin et al. [41] included DNA barcoding, phylogeny, and phylogeography of *Globodera* species from 23 countries. This study provided a comprehensive phylogenetic analysis of 455 ITS rDNA, 219 COI, and 164 cytb gene sequences [41]. LAMP assays for rapid detection of *G.pallida* was recently developed by Camacho et al. [42].

The genome-wide allele frequency and fixation index (F_{st}) analyses conducted by Wasala et al. [43] on *G. pallida* populations in Idaho indicated that the infestation likely resulted from a single introduction.

Pathogenicity: Yield losses caused by the white (pale) potato cyst nematode (*Globodera pallida*) can reach up to 80% of the total production under high infestation and continuous potato culture, especially in the temperate areas [41]. No yield losses caused by *G. pallida* in Idaho were documented, as in other countries, because the infestation was detected and addressed before the pest level could reach the threshold for significant crop yield loss [43].

Diagnosis (see Table 4).

Table 4. Morphometrics for *Globodera* Behrens, 1975 after Skantar et al. [40] (courtesy of Journal of Nematology).

Species Name from Original *Heterodera* Description	J2 Stylet (μm)	Cyst, Number of Cuticular Ridges from Anus-Vulva	Cyst Anus-Vulva Distance (μm)	Granek's Ratio
G. rostochiensis				
(Wollenweber, 1923) [44]	19–23 (22)	12–31 (>14)	37–77 (>55)	1.3–9.5 (>3)
(Manduric et al., 2004) [45]	19.3–24	12–28	38–149	1.7–6.7
Composite	19–24	12–31	37–149	1.9–9.5
G. pallida				
(Stone, 1973) [46]	22–24 (23.8)	8–20 (<14)	22–67 (<50)	1.2–3.5 (<3)
(Manduric et al., 2004) [45]	21.1–25.5	9–26	28–88	1.0–6.5
Composite	21.1–25.5	7–26	22–88	1–6.5
G.tabacum				
(Lownsbery, 1954) [47]; (Miller and Gray, 1968) [48]; (Miller and Gray, 1972) [49]	19–28 (23–24)	10–14	28–85	1–4.2 (<2.8)
G.achilliae				
(Golden and Klindic, 1973) [50]	24–26 (25)	4–5	22–34 (27)	1.5–1.9 (1.6)
(Brzeski, 1988) [51]	24–26.5 (25)	-	12–42 (24)	0.3–1.9 (1.2)
(Skantar et al.,2006) [40]	-	5–11 (8 ± 1.7)	25–60 (21.5 ± 2.6)	1.2–2.1 (1.5 ± 0.3)
G. artemisiae				
(Eroshenko and Kazachenko, 1972) [52]	18–29 (23)	5 [a]	25–42 (32 [b])	0.8–1.7 (1.0)

[a] New: Measured from the original photograph. [b] Translated from Russian: "Anus to outer edge of fenestra".

1.4. Globodera rostochiensis (Wollenweber, 1923) Behrens, 1975

- *Common name*: Golden (yellow) potato cyst nematode
- *Type plant host*: *Solanum tuberosum* L.
- *Type locality*: Epworth, Lincolnshire, Eastern England
- *First U.S. report*: 1941, Hicksville, NY

Measurements: (after Golden and Ellington [3]; Subbotin, 2010 [53]).

Female: n = 50; length (including neck) 0.52 mm (0.42–0.64); width 0.34 mm (0.27–0.43); L/W ratio 1.5 (1.2–2.0); stylet 23 μ (22–24); outlet of dorsal esophageal gland 6.2 (5.8–7.0).

Male: n = 50; length 1.08 mm (0.89–1.27); a = 27 (22–36); b = 5.9 (4.9–7.3); c = 267 (161–664); stylet 26 μ. (25–27); outlet of dorsal esophageal gland 6.4 μ, (5.3–7.0); spicules 35 μ (32–39); gubernaculum 12 μ (10–14); tail 4.4 μ (1.7–6.7).

Juveniles: n = 50; length 0.43 mm (0.37–0.47); a = 19 (16–23); b = 2,3 (2.2–2.5); c = 8 (7–9); stylet 22 (21–23) μm; outlet of dorsal esophageal gland 5.5 (5.0–6.7) μm; tail 51 (44–57) μm;

hyaline tail terminal 24 (18–30) µm; caudal ratio A = 3.4 (2.8–4.4); caudal ratio B = 10.8 (5.5–17.0).

Cyst: n = 50; length (including neck) 0.68 mm (0.45–0.99); width 0,54 mm (0.25–0.81); L/W ratio = 1.27 (1.0–1.8); fenestra diameter 15 (8–20) µm; distance from anus to nearest edge of fenestra 68 (29–116) µm; Granek's ratio 4.5 (2.0–7.0).

Description (modified after Golden and Ellington [3]; Subbotin 2010 [53]).

Female: White subspherical shaped body with a long, protruding neck. Thick cuticle with punctuations near or beneath the surface. Head bearing two annules, slightly set off. Well-developed stylet and basal knobs oriented posteriorly. Spherical large median bulb. Excretory pore prominent, approximately 105–175 µm from the anterior end. Vulva small, between 7 and 14 µm in length and between 5 and 11 µm in width, and a small vulva slit between 6 and 11 µm in length. Anal opening much smaller than the vulva opening, located between 39 and 80 µm from the nearest edge of the vulva.

Male: Vermiform, tapering slightly at both extremities. Head slightly set off with six annules. Stylet very well developed, with prominent knobs. Median bulb located between 85 and 112 µm from the anterior end. Excretory pore located two annules posterior to the hemizonid. Four lines in the lateral field. Spicules slightly arcuate, with rounded tips. Tail short.

Juvenile: Vermiform, tapering slightly at both extremities but much more posteriorly. Head slightly set off with five annules. Stylet well developed, with prominent knobs. Excretory pore posterior or adjacent to hemizonid. Four lines in lateral field. Tail tapering to small with a rounded tail terminus.

Cyst: Brown in color with ovate to spherical shape. Protruding neck. Cysts circumfenestrate and without bullae. Fenestra much larger than the anus. Ridge-like to wavy line cyst wall pattern with lines going latitudinally around the body. Punctation present most of the times but variable in intensity and arrangement.

U.S. Distribution: Since its first report by Cannon [54,55] in 1968, the spread of this species is still limited to a few counties in New York state APHIS (Figure 5) [56].

Molecular characterization: This species was characterized by using multiplex polymerase chain reaction of the internal transcribed spacer (ITS) rDNA region, ITS1 and 2, and mitochondrial DNA cytochrome oxidase subunit I (COI) or by DNA barcoding based on the 18 S rDNA gene and ITS1 region of the rDNA [5,57–59]. LAMP assays were developed for *G. rostochiensis* population from Belgium and Netherlands [60,61].

Pathogenicity: *G. rostochiensis* maintains an invasive status in potato-producing countries where its presence has not been reported. Since 1941, when it was first found in the U.S., federal, state, and local governments tried to eliminate and stop the spread of this pest. If left uncontrolled, this nematode can cause 100% loss in potato yields [62]. Yield losses caused by the golden potato cyst nematode were up to 70% of the total production in the New York field where this pest was first reported in the U.S. [62]. Preliminary pathogenicity tests, and observations of growth and yield losses caused by the golden nematode in infested fields on Long Island indicated the serious nature of this pest.

Diagnosis: The morphological characteristics of cysts commonly used for the identification of this species include cyst shape; characteristics of a cyst terminal cone, including the nature of fenestration; cyst wall pattern; anal–vulval distance; number of cuticular ridges between anus and vulva; and Granek's ratio. The second-stage juvenile morphologies critical for identification were the following: body and stylet length, shape of stylet knobs, shape and length of tail and hyaline tail terminus, and number of refractive bodies in the hyaline part of tail [5].

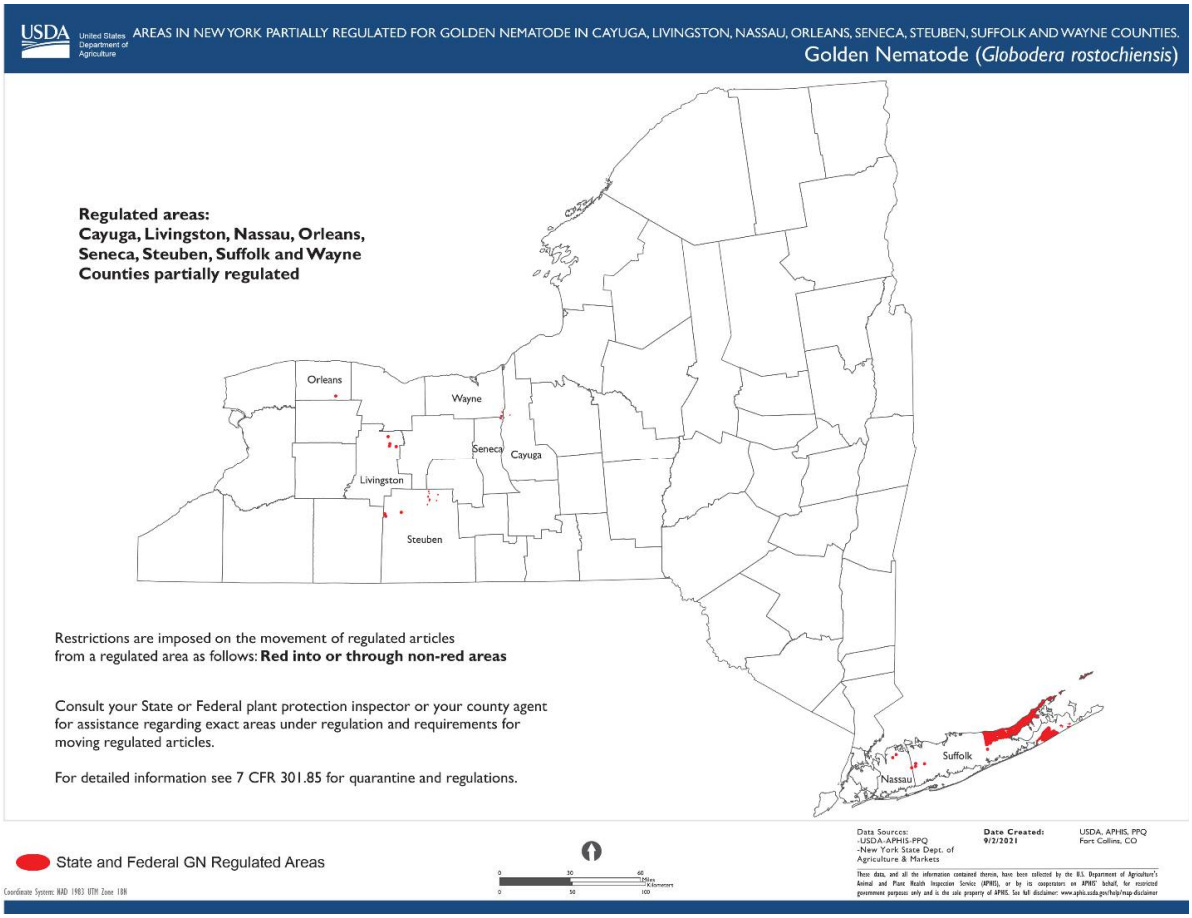

Figure 5. Continental U.S. distribution of *Globodera rostochiensis* (source, USDA, APHIS).

1.5. Heterodera glycines Ichinobe, 1952

- *Common name*: Soybean cyst nematode
- *Type plant host*: *Glycine max*, soybean
- *Type locality*: Obihiro-shi, Hokkaido, Japan
- *First U.S. report*: 1955, NC

Measurements: (see Table 5).

Table 5. Morphometrics of *Heterodera glycines* Ichinobe, 1952 cysts and juveniles. All measurements are given in µm.

	Cyst Measurements after Hirschmann [63]	Cyst Measurements after Burrows and Stone [64]	Cyst Measurements after Wang et al. [65]	Juvenile Measurements after Hirschmann [63]	Juvenile Measurements after Burrows and Stone [64]	Juvenile Measurements after Wang et al. [65]
Character	n = 100	-	n = 5	n = 150		n = 15
Body length	580 (340–920)	340–920	696 (520–866)	440 ±6.7 (375–490)	440 (375–490)	438.5 (381–510)
Body width	360 (200–560)	-	399.8 (320–495)	-	-	-
Length/width	1.2–2.1	1.19–2.05	1.7 (1.4–2.1)	-	-	-
Vulva slit	49.7 (43–56)	49.7 (43–56)	48.2 (42–52)	-	-	-
Fenestra length	53.7 (37–65)	53.7 (37–65)	58.4 (52–65)	-	-	-
Fenestra width	40.5 (33–48)	40.5 (33–48)	37.4 (32–40)	-	-	-
Vulva to anus distance	67.5 (59–77)	-	-	-	-	-
Underbridge			80 (70–110)	-	-	-
Stylet length	-	-	-	23.0 ± 0.1 (22–24)	23.0 (22.0–24.0)	23.8 (22.5–25)
Tail length	-	-	-	50.4 ± 1.0 (42–59.4)	50.4 (42.0–59.4)	47.3 (42–50)
Hyaline tail terminal length	-	-	-	26.6 ± 0.7 (20.0–33.0)	26.6 (20.0–33.0)	25.1 (22.5–27.5)

Description (modified after Thorne [30], Hirschmann [63], and Subbotin [66]).

Female: Most of the time, females are lemon-shaped to rounded, with protruding neck and vulval cone. Thick cuticle with zigzag striae in mid-body. Well-developed stylet, median bulb large, subspherical. Excretory pore located at the base of neck within a depression appearing smooth. Vulva is a transverse slit. Anus is a small slit. Females develop an egg sac that contains up to 200 eggs.

Cyst: Dark brown in color at maturity, lemon-shaped, sometimes round with a protruding neck and cone. Cyst wall with a rugose pattern formed by many zigzag lines without order. Ambifenestrate. Vulval length averaging 49.7 (43–56) µm, and vulval bridge bears vulval slit and divides the fenestra into two semifenestrae. Bullae well developed, located at or anterior to underbridge, extending into vulval cone. Underbridge well developed.

Male: Vermiform, with a length averaging 1.3 (1.1–1.4) mm. Labial region offset with four or five annuli. Stylet well developed, with big, rounded knobs projecting laterally to anteriorly. Median bulb has a slender ellipse shape. Esophageal gland nuclei present, about one body diameter apart. Hemizonid found about six annules anterior to excretory pore. Short, bluntly rounded tail with length less than 10% of body diameter. Spicule is bidentate, curved ventrally. Gubernaculum slightly curved.

Juvenile: Vermiform, with an average length of 439.6 (373.0–490.0) µm. Labial region offset with three to four annuli. Stylet robust, with knobs slightly rounded, projected anteriorly. Hemizonid found adjacent to excretory pore, about two annuli long. Four lines in the lateral field. Tail tapering uniformly with a rounded tail terminus. Long hyaline portion, occupying almost half of the tail.

U.S. Distribution (see Figure 6).

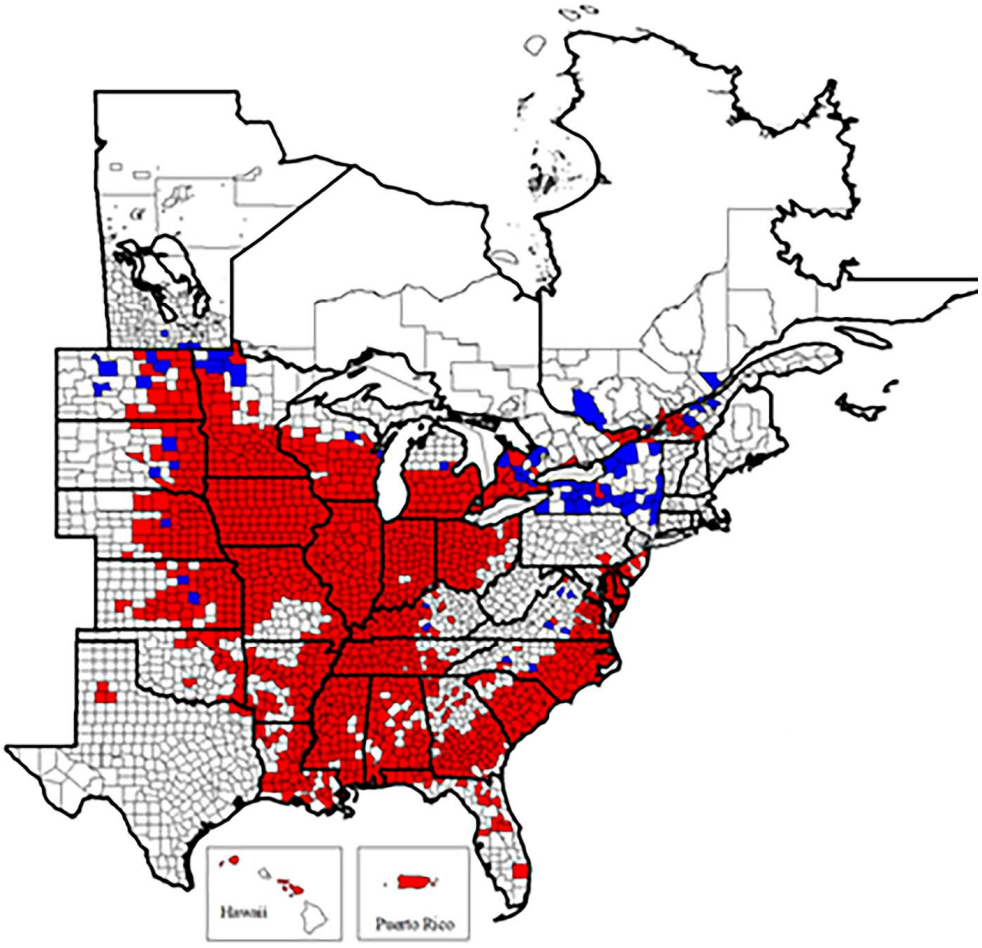

Figure 6. Continental U.S. distribution of *Heterodera glycines* (source, Tylka and Marett, courtesy of Plant Health Progress) [9].

Molecular characterization: PCR-based identification methods of the soybean cyst nematode have been developed based on ribosomal DNA of ITS,28 S and *COI* regions [65–68]. Additionally, PCR species-specific primers for *H. glycines* were developed by several researchers [66,68].

Pathogenicity: The soybean cyst nematode has a significant negative impact on soybean-producing areas of the U.S. and Canada [9,69,70]. In the U.S. alone, this pathogen caused estimated yield losses totaling nearly USD 32 billion from 1996 through 2016, which is more than USD 1.5 billion annually [9,71]. From 2003 to 2005 alone, this nematode caused 2–3 million tons of yield loss annually [66]. In Japan, yield losses have been estimated to be between 10 and 79% [66]. The widespread distribution and the resilience of this pest could lead to great yield losses [9,72]

Diagnosis (modified after Thorne [30], Hirschmann [63], Subbotin [66], and Handoo and Subbotin [67]).

This species can be differentiated from *H. trifolii* based on the length of the juveniles, which are smaller when compared to *H. trifolii* (439.6 vs. 496.6 µm). The dorso-esophageal opening is 4.0 µm behind the stylet vs. 7.3 µm in *H. trifolii*. The shape of the knobs are somewhat rounded instead of forward-pointing as in *H. trifolii*. From *H. medicaginis*, it differs by having a shorter J2 stylet (21–23 vs. 25 µm) and a shorter tail (39–51 vs. 52 µm). It differs from *H. schachtii* by having a shorter average stylet length in J2 (21–23 vs. 25–26 µm), in the shape of the J2 knobs (slightly convex vs. moderately or strong concave), and by having a longer average fenestra length (34–58 vs. 35–38 µm). From *H. daeverti*, it differs by having a shorter average stylet in J2 (21–23 vs. 25–26 µm) and shorter tail (39–51 vs. 54–57 µm) and hyaline tail terminus (22–30 vs. 30–33 µm).

1.6. Meloidogyne chitwoodi Golden, O'Bannon, Santo & Finley, 1980

- *Common name*: Columbia root-knot nematode
- *Type plant host*: Solanum tuberosum L. potato
- *Type locality*: Quincy, Washington, USA

Measurements: (modified after Golden et al. [73]).

Female: n = 60; the average females length is 591 ± 60 (430–740) µm; a = 1.4 ± 0.2 (1–1.8); body width 422 ± 42 (344–518) µm, stylet length 11.9 ± 0.3 (11.2–12.5) µm; stylet knobs width 3.8 ± 0.3 (3.4–4.3) µm; DGO = 4.2 ± 0.6 (3.4–5.5) µm; anterior end to median bulb valve distance 63 ± 7 (52–80) µm; anterior end to excretory pore distance 18 ± 5 (10–27) µm; vulva slit 27 ± 3 (19–32) µm; vulva to anus distance 18 ± 2 (13–22) µm.

Male: n = 30; length 1068 ± 100 (887–1268) µm; a = 36 ± 4 (28–46); b = 7.2 ± 1 (6–9); c = 162± 20 (140–226); body width 30 ± 3.9 (22–37) µm; diameter of labial region 18.3 ± 0.2 (18.1–18.5); DGO = 3.0 ± 0.4 (2.2–3.4) µm; anterior end to median bulb valve distance 71 ± 5 (61–77) µm; spicule length 27 ± 1.2 (26–29) µm; gubernaculam length 7.7 ± 0.6 (6.5–8.2) µm; tail length 6.8 ± 0.9 (4.7–9.0) µm.

Juvenile: n = 60; length 390 ± 16 (336–417) µm; a = 27.5 ± 1.2 (24.5–29.8); b = 3.6 ± 0.2 (3.3–3.8); c = 8.9 ± 0.4 (7.9–9.6); body width 14.2 ± 0.6 (12.5–15.5) µm; height of labial region 2.3 ± 0.2 (1.7–2.6) µm; diameter of labial region 5 ± 0.2 (4.7–5.2) µm; stylet length 9.9 ± 0.3 (9.0–10.3) µm; DGO = 3.2 ± 0.2 (2.6–3.9) µm; anterior end to median bulb valve distance 51 ± 3 (43–56) µm; tail length 43 ± 1.8 (39–47) µm; hyaline tail region 11 ± 1 (8.6–13.8) µm.

Description (modified after Subbotin [13], Golden et al. [73], and Eisenback and Triantaphyllou [74]).

Female: The females are mostly found in the galls, and the egg masses protrude from the root tissue. Body pearly white, pear-shaped, with slight posterior protuberance visible occasionally, and with distinct neck situated anteriorly on a median plane with terminal vulva. Vulva appears sometimes to be located on a slight posterior protuberance. Several small vesicles or vesicle-like structures usually present within median bulb and clustered around lumen anterior to valve plates of median bulb. Labial region with distinct but weak labial framework, offset from neck but variable in exact shape, bearing a labial cap and usually one labial annulus. Excretory pore clearly visible and commonly located at a

distance equal to about 1.5 stylet lengths from anterior end. Stylet length between 11 and 12.5 (12) µm but strong, having a dorsal curvature and rounded knobs sloping posteriorly. The distance of the DEGO to the base of the stylet between 3.5 and 5.5 (4.2) µm. The female stylet of this species is morphologically unique and very useful for species identification. The morphology of the stylet knobs is characteristic for the species; they are small, irregular in outline, indented medially, and taper onto the shaft. Perineal pattern is round to oval, with distinctive striae around and above anal area being broken, curved, twisted, or curled. Dorsal arch variable, ranging from low and round to high and sometimes squarish, like *M. incognita*. The striae in the dorsal area are more twisted when compared with those from the ventral area. Striae further away from the perineal area are smoother. Sometimes punctations visible in a small area between the anus and first inner striae (tail terminus) or the striae are absent. Vulva sunken in an area variable in shape and devoid of striae. Lateral striae may bend toward the vulva.

Male: Slender, vermiform, tapering slightly at both extremities. The shape of the male head is characteristic for the species. Labial disc large with median lips are fused into a labial cap. However, the labial disc slightly higher than median lips and post-labial annulus lacking annulations, and the posterior edges are irregular in outline. In labial region, two large, not well-delimited lateral lips that may have irregular outlines are marked by additional short grooves. Cuticular annuli distinct, more prominent a short distance from either end. The stylet is long and thin. The stylet opening is approximately 3 µm from the tip. Four lines present in the lateral field, the center band smaller than outer two. Areolation evident with SEM but difficult to observe under light microscope. Testis one or two. Spicules arcuate, under SEM can be seen to have dentate tips ventrally. Phasmids located at or anterior to cloacal aperture. Tail short, rounded.

Juvenile: Vermiform, small, tapering at both extremities but mostly posteriorly. The shape of the head of juveniles is not diagnostic for the species. Labial region not offset, with weak framework, bearing a labial disc and a large post-labial annulus lacking striations. The labial disk and medial lips are fused to form the head cap. The head cap appears anchor-shaped. The stylet of *M. chitwoodi* juveniles is useful for species identification. The anterior margins of the stylet knobs are indented and round to irregular and appear stippled. Cuticular annulation on most of body is very fine. Lateral field with four lines, areolated. Cephalids indistinct or not seen. Phasmids small, difficult to see, located in anterior one-third of the tail. Rectum not inflated. Tail ends in a broad, blunt tip, with the blunt hyaline region remaining almost the same diameter for its length and with little or no taper. The hyaline tail terminus is short and clearly delineated.

U.S. Distribution: see Figure 7.

Figure 7. Continental U.S. distribution map of *Meloidogyne chitwoodi* (adapted from CABI-ISC) [26].

Molecular characterization: Molecular approaches based on PCR, PCR-RFLP of ITS region, ribosomal DNA of the intergenic spacer (IGS) region, and mitochondrial DNA and ribosomal RNA regions were successfully developed to distinguish this species from other closely related species. A simple ITS PCR-RFLP differentiation method was developed by Zijlstra [75,76] for *M. chitwoodi*, *M. fallax*, *M. hapla*, *M. incognita*, and *M. javanica* [13]. Later on (2000), Zijlstra [77] used a highly sensitive PCR method with species-specific SCAR primers. In 2002, Wishart et al. [78] designed a sensitive PCR method based on species-specific primers from ribosomal IGS regions [15]. MtDNA and rRNA genes for *M. chitwoodi* were sequenced by several authors [13]. LAMP assays for *M.chitwoodi* were designed recently by Zhang and Gleason [79].

Pathogenicity: This species is a major economic potato pest in Pacific Northwest U.S. [73,74]. It is predicted to cause annual losses of approximately USD 40 million if not treated [13]. The major damage that this nematode causes to potato tubers is a blemish that lowers the tuber marketability [80].

Diagnosis: Morphologically, this species is close to *M. hapla,* but it can be distinguished by differences in the perineal pattern, which has broken, curved, twisted, or curled striae around and above the anal area; by the sunken vulva; and by the presence of vesicles or vesicle-like structures in the median bulb of the females and by the tail shape in juveniles [73]. *M. fallax* is another close species to *M. chitwodi*, but the latter can be differentiated by having a shorter stylet length (16–19 vs. 19–21 µm) in males and a shorter J2 tail length (39–51 vs. 46–57 µm) and hyaline region (8–14 vs. 12–16 µm) [13,15]. Molecularly, *Meloidogyne chitwoodi* can be distinguished from *M. fallax* and other species by the ITS rRNA and *COI* gene sequence.

1.7. Meloidogyne enterolobii Yang & Eisenback, 1983

- *Common name*: Guava root-knot nematode
- *Type plant host*: *Enterolobium contortisiliquum* (Vell.) Morong, pacara earpod tree.
- *Type locality*: Hainan Island, Hainan Province, China.
- *First U.S. report*: 2001, FL.

Measurements: (modified after Eisenback and Triantaphyllou [74].

Female: n = 20; the average females body length is 735 ± 92.83 (541.3–926.3) µm; a = 1.25 ± 0.23 (0.97–1.94); body width 606.8 ± 120.52 (375.7–809.7) µm, neck length 218.4 ± 74.16 (114.3–466.8); stylet length 15.1 ± 1.35 (13.2–18.0) µm; stylet knobs width 4.9 ± 0.39 (4.1–5.6) µm; stylet knobs height 2.4 ± 0.26 (1.9–3.1) µm; DGO = 4.9 ± 0.78 (3.7–6.2) µm; excretory pore to head end 62.9 ± 10.5 (42.3–80.6) µm; interphasmidial distance 30.7 ± 4.78 (22.2–42.0) µm; vulva length 28.7 ± 1.76 (25.3–32.4) µm; vulva to anus distance 22.2 ± 1.76 (19.7–26.6) µm; number of body annules from head end to excretory pore 36 ± 6.73 (24–48).

Male: n = 20; body length 1599.8 ± 159.91 (1348.6–1913.3 µm; a = 37.9 ± 3.15 (34.1–45.5); c = 131.6 ± 24.15 (72.0–173.4); body width 42.3 ± 3.56 (37.0–48.3) µm; stylet length 23.4 ± 0.96 (21.2–25.5) µm; stylet knob height 3.3 ± 0.33 (2.6–3.9) µm; stylet knob width 5.4 ± 0.3 (4.5–5.8) µm; DGO= 4.7 ± 0.41 (3.7–5.3) µm; excretory pore to head end 178.2 ± 11.16 (159.7–206.2) µm; spicule length 30.4 ± 1.16 (27.3–32.1) µm; gubernaculum length 6.2 ± 0.96 (4.8–8.0) µm; tail length 12.5 ± 2.24 (8.6–20.2) µm, testis length 810.1 ± 24.15 (597.0–1055.0).

Juvenile: n = 30; body length 436.6 ± 16.61 (405.0–472.9) µm; a = 28.6 ± 1.88 (24.0–32.5); c = 7.8 ±0.65 (6.8–10.1); body length/head end to posterior end of metacorpus 6.5 ± 0.18 (6.2–6.9) µm; body width 15.3 ± 0.89 (13.9–17.8) µm; excretory pore to head end distance 91.7 ± 3.34(84.0–98.6) µm; stylet length 11.7 ± 0.45 (10.8–13.0) µm; stylet knobs width 2.9 ± 0.25 (2.4–3.4) µm; stylet knobs height 1.6 ± 0.13 (1.3–1.8) µm; DGO = 3.4 ± 0.33 (2.8–4.3) µm; tail length 56.4 ± 4.48 (41.5–63.4) µm.

Description (modified after Eisenback and Triantaphyllou [74] and Subbotin et al. [13]).

Female: Body white, pear-shaped to globular, variable in size, with prominent neck variable in size, without posterior protuberance. Labial region not distinctly offset from neck. Labial disc and median lips fuse to form head cap. Hexaradiate labial framework distinct but weak; vestibule and vestibule extension prominent. Cephalids and hemizonid

not observed. Position of excretory pore variable, often near median bulb. Cuticular body annulations becoming progressively finer posteriorly. Stylet slender; conical portion slightly curved dorsally, tapering toward tip; cylindrical shaft, posterior end often enlarged. Stylet knobs offset from shaft, distinct from each other, and divided longitudinally by groove so that each knob appears as two. DGO found at 4–6 µm from the stylet knobs base. Dorsal gland ampula large. Subventral gland orifices branched, located immediately posterior to enlarged lumen lining of median bulb; subventral gland ampulla small but distinct. Pharyngeal gland comprised of one large uninucleate dorsal pharyngeal gland lobe; two small nucleated subventral pharyngeal gland lobes usually posterior to dorsal gland lobe but variable in position, shape, and size. Perineal pattern usually oval-shaped with coarse and smooth striae, dorsal arch moderately high to high, often rounded, nearly square in some specimens. Lateral lines not distinguishable. Perivulval region usually free of striae; however, striae may occur on lateral sides of vulva. Striae present on ventral area of pattern generally finer and smoother. Tail tip visible; large phasmidial ducts.

Male: Vermiform body, tapering at both ends. Tail end more rounded than anterior end, twisting through 90° in heat killed specimens. In lateral view, labial cap high and rounded, labial region only slightly offset from body. Hexaradiate labial framework moderately developed, vestibule and extension distinct. In SEM, stoma slit-like, prestoma hexagonal, surrounded by pit-like openings of six inner labial sensilla. Labial disc and median labials fused, forming elongate labial cap and labial disc slightly elevated above median labials. Four labial sensilla marked on median labials by shallow cuticular depressions. Amphid openings slit-like. Lateral labials absent. Head region not annulated. Body annules easily distinguishable. Four lines in the lateral field, with two lines beginning near level of stylet knobs; two additional lateral lines beginning near the level of the median bulb. Areolated lateral field, encircling tail. Stylet well developed, cone straight, pointed, opening located several micrometers from tip. Shaft cylindrical, with large rounded basal knobs, distinctly offset from shaft, in some specimens each knob divided longitudinally by a groove so that each knob appears as two, but not as pronounced as in female. Procorpus distinct. Median bulb elongated, oval-shaped with enlarged cuticular lumen lining. Pharyngo-intestinal junction indistinct, at level of nerve ring. Gland lobe variable in length, with two nuclei. Excretory pore distanced from anterior end, terminal duct long. Hemizonid located 2–4 annules anterior to excretory pore. One or two testes, usually outstretched. Spicules arcuate, with rounded base, single tip. Gubernaculum short and simple. Tail short and rounded. Phasmids small, pore-like, at level of cloacal aperture.

Juvenile: Body vermiform, tapering at both ends with very long, narrow tail. Anterior end truncate. Labial region only slightly offset from body. Vestibule and extension more developed than remainder of hexaradiate labial framework. In SEM, stoma slit-like, located in oval-shaped prestoma, surrounded by six pore-like openings of inner labial sensilla. Median labials and labial disc dumbbell-shaped in face view. Rounded labial disc slightly raised above medial lips. Large and triangular lateral lips, lower than labial disc and medial lips. Posterior edge of one or both lateral lips may fuse with head region in some specimens. Elongate amphidial apertures located between labial disc and lateral lips. Head region without annulations. Body annules distinct and narrow. Lateral field with four lines, appearing near level of procorpus as two lines. Third line begins near median bulb and quickly splits to form four lines, running entire length of body. Hyaline tail terminus irregularly areolated. In LM stylet delicate. Cone straight, narrow, sharply pointed, shaft becomes slightly wider posteriorly. Large, rounded stylet basal knobs separate from each other, offset from shaft. Distance from base of the stylet to dorsal esophageal gland orifice about 2.8–4.3 µm long. Procorpus faintly outlined, median bulb oval-shaped with enlarged lumen lining, isthmus not clearly defined pharyngo-intestinal junction hard to observe. Gland lobe variable in length, with three equally sized nuclei, overlapping intestine ventrally. Excretory pore distinct, hemizonid 1–2 annuli anterior to excretory pore, 3–5 annuli long. Cuticle slightly raised over hemizonid. Tail very thin, annuli increasing in size, become more irregular posteriorly. Hyaline tail terminus clearly defined; tail tip

broad, bluntly rounded. Rectum dilated. A few fat droplets may occur in hyaline terminus. Hardly distinguishable small phasmids located posterior to anus.

U.S. Distribution (see Figure 8).

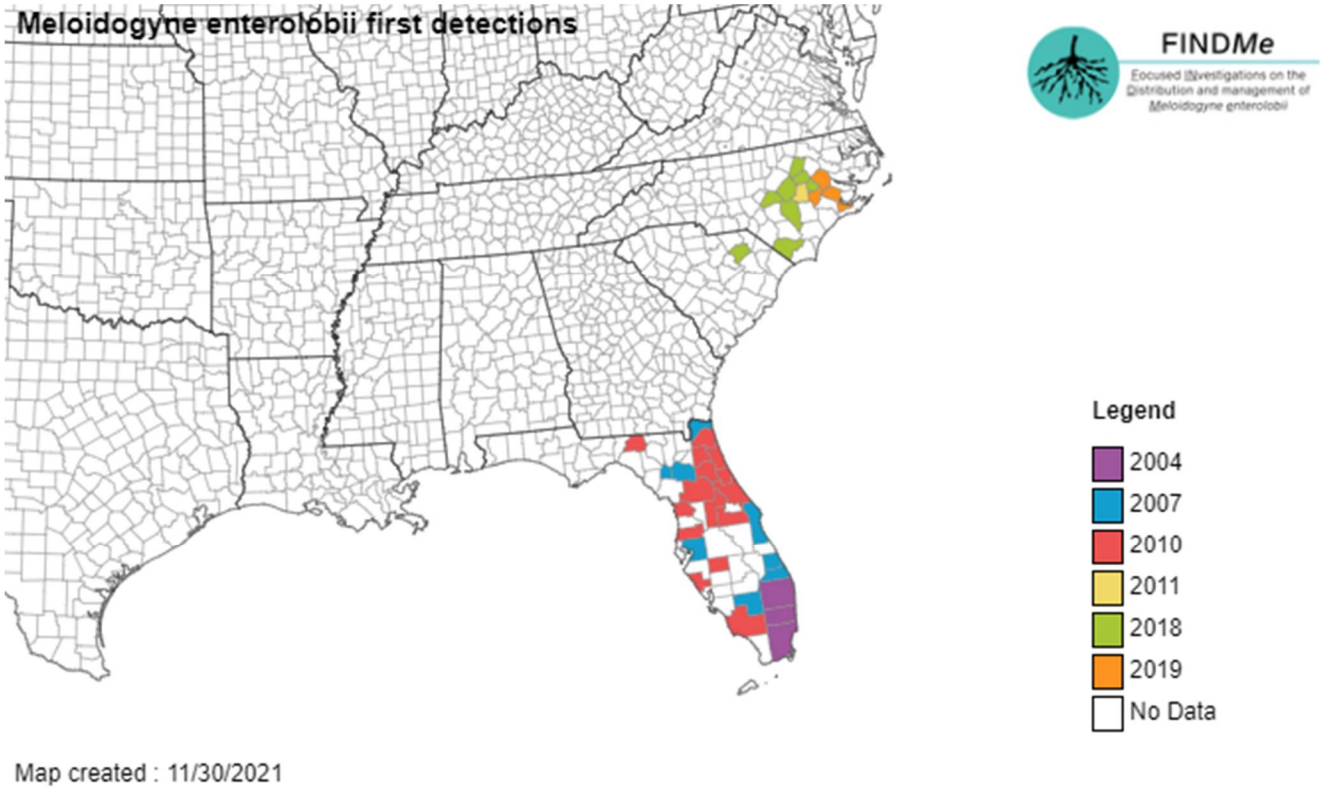

Figure 8. Continental U.S. distribution map of *Meloidogyne enterolobii* (source, FIND*Me*.org) [81].

Molecular characterization: Subbotin et al. [13] outlined molecular techniques used in the identification of *M. enterolobii*, including sequencing of the IGS rRNA gene [82]; intergeneric mitochondrial region between the *COII* and lRNA genes [18,83,84]; ITS rRNA [18]; *COI*, *COII*, partial 28 S rRNA, and 18 S rRNA genes [85]; conventional PCR with specific primers [86,87]; loop-mediated isothermal amplification (LAMP) [88,89]; and real-time PCR with specific primers [90,91]. Recombinase polymerase amplification assays were also developed to target the IGS rRNA gene of *M. enterolobii* [92].

Pathogenicity: This species is not yet a regulated pest in the U.S. However, it is considered an emerging and a highly virulent root-knot nematode species that could be devastating to specialty crops in the U.S. [93]. This species is more efficient at breaking resistance than other tropical root-knot species such as *M. arenaria*, *M. javanica*, or *M. incognita* [16]. *M. enterolobii* is considered as a quarantine pest in different countries and listed as an EPPO A2 pest list for the EPPO region [13,16].

Diagnosis: Morphologically, this species can be separated from other described species by the form of the perineal pattern, the stylet morphology, and the position of excretory pore in female specimens. The morphology of the head in male and juveniles as well as the tail morphology in juveniles are also diagnostic characteristics. This species differs from *M. incognita* by several morphological characteristics. Stylet knobs are rounded, slightly sloping posteriorly, and divided longitudinally by distinct grooves so that each knob appears as two in the female specimens. The DGO distance is much longer in *M. enterolobii* (3.7–6.2 µm) when compared to *M. incognita* (2–4 µm). The female perineal pattern is oval-shaped, with the dorsal arch being moderately high to high and most of the times rounded. In the male specimens, the DGO distance is longer than in *M. incognita* (3.7–5.3 vs. 1.7–3.5 µm). The juvenile specimens of *M. enterolobii* have longer body when compared

to *M. incognita*. This species differs from *M. arenaria* by body length of the juveniles and from *M. javanica* by male stylet length and J2 body length. The nematode formerly known as *M. mayaguensis* is now recognized as a junior synonym of *M. enterolobii* [94].

1.8. Meloidogyne fallax Karssen, 1996

- *Common name*: False Columbia root-knot nematode
- *Type plant host*: *Solanum lycopersicum* L., tomato
- *Type locality*: Limburg, Netherlands
- *First U.S. report*: San Francisco County, CA

Measurements (modified after Subbotin et al. [13] and Karssen [95]).

Female: n = 30; body length 491.3 ± 74.9 (404.1–720.3) µm; body width = 361.6 ± 57.7 (256.2–464.1) µm; stylet 14.5 ± 0.4 (13.9–15.2) µm; stylet knob height 2.3 ± 0.3 (2.0–2.5) µm; stylet knob width 4.2 ± 0.3 (3.8–4.4) µm; DGO 4.3 ± 0.5 (3.8–6.3) µm; anterior end to excretory pore distance 22.5 ± 5.3 (12.6–32.9) µm; vulval slit length 24.7 ± 1.8 (20.2–28.4) µm; vulva–anus distance 15.9 ± 1.8 (12.6–19.0) µm; a = 1.4 ± 0.3 (0.9–2.0); EP/ST = 1.6 (estimated from three drawings).

Male: n = 30; body length 1171 ± 193.6 (736.2–1520.1) µm; body width 30.6 ± 2.1 (27.2–43.8) µm; labial region height 4.6 ± 0.3 (4.4–5.1) µm; labial region diameter 10.7 ± 0.7 (9.5–12.0) µm; stylet 19.6 ± 0.8 (18.9–20.9) µm; stylet knob height 3.0 ± 0.3 (2.5–3.2) µm; stylet knob width 4.9 ± 0.4 (3.8–5.1) µm; DGO 4.4 ± 0.7 (3.2–5.7) µm; anterior end to median bulb valve distance 65.4 ± 4.1 (58.8–72.7) µm; anterior end to excretory pore distance 120.9 ± 11.4 (94.8–139.9) µm; tail length 9.2 ± 1.4 (7.6–12.1) µm; spicules 26.6 ± 2.0 (22.1–29.7) µm; gubernaculum 7.7 ± 7 0.5 (7.0–8.5) µm; a = 38.2 ± 6.8 (21.2–53.5); c = 127.8 ± 28.5 (82.7–201.7); T = 42.4 ± 8.4 (24.4–62.1).

Juvenile: n = 30; body length 403.2 ± 15.2 (381.4–435.2) µm; body width 14.3 ± 0.7 (13.3–16.4) µm; labial region height 2.7 ± 0.4 (1.9–3.2) µm; labial region diam. 5.5 ± 0.3 (5.1–6.3) µm; stylet 10.8 ± 0.4 (10.1–11.4) µm; stylet knob height = 1.5 ± 0.3 (1.3–1.9) µm; stylet knob width 2.3 ± 0.3 (1.9–2.5) µm; DGO 3.5 ± 0.3 (3.2–3.8) µm; anterior end to median bulb distance 48.0 ± 3.5 (44.2–54.4) µm; anterior end to excretory pore distance 69.1 ± 3.4 (63.2–77.1) µm; tail length 49.3 ± 2.2 (46.1–55.6) µm; hyaline tail region 13.5 ± 1.0 (12.2–15.8) µm; a = 28.1 ± 1.7 (23.8–40.4); c = 8.2 ± 0.5 (6.9–8.6).

Description (modified after Subbotin et al. [13] and Karssen [95]).

Female: Body annulated, pearly white, globular to pear-shaped, with slight posterior protuberance and distinct neck region projecting from body axis at an angle of up to 90° to one side. Head region offset, with one or two annules. Distinct head cap, variable in shape with a slightly elevated labial disc. Cephalic framework weakly sclerotized; vestibule extension distinct. Stylet cone dorsally curved with knobs large, rounded to transversely ovoid, leaning slightly posteriorly from shaft. Excretory pore found between anterior end and median bulb level. One or two large vesicles and several smaller ones located along lumen lining. Pharyngeal glands variable in size and shape. Perineal pattern ovoid to oval-shaped, sometimes rectangular. Dorsal arch ranging from low to moderately high, having coarse striae. Tail terminus indistinct without punctations. Phasmids small and difficult to observe. Perivulval area devoid of striae. Lateral lines indistinct, appearing as a weak indentation under SEM, increasing towards tail terminus region and resulting in a relatively large area without striae. Ventral pattern region oval to angular shaped; striae moderately coarse.

Male: Body vermiform, slightly tapering anteriorly, bluntly rounded posteriorly. Cuticle with distinct transverse striae. Four lines in the lateral field, the outer bands irregularly areolated, a fifth, broken, longitudinal incisure sometimes present near mid-body. Slightly offset head, with a single post-labial annule usually partly subdivided by a transverse incisure. Labial disc rounded, elevated, and fused with medial lips. Medial lips crescent shaped with raised edges at lateral sides. Four small labial sensilla marked by cuticular depressions on medial lips. Amphidial openings appearing as elongated slits between labial disc and medium-sized lateral lips. Cephalic framework moderately sclerotised,

vestibule extension distinct. Stylet cone straight, with large rounded basal knobs, offset from shaft. Pharynx with slender procorpus, median bulb oval-shaped with pronounced valve. Ventrally overlapping pharyngeal gland lobe of variable length. Hemizonid, 2–3 µm long, two to four annuli anterior to excretory pore. Testis usually long, monorchic, with reflexed or outstretched germinal zone. Tail short and twisted. Spicules slender, curved ventrally and gubernaculum slightly crescent shaped. Phasmids located anterior to cloacal aperture.

Juvenile: Vermiform, moderately long body, tapering at both ends but posteriorly more so than anteriorly. Body annules are small but distinct. Four lines in the lateral field; not areolated. Head truncated, slightly offset from body. Head cap low and narrower than the labial region. Cephalic framework weakly sclerotized, vestibule extension distinct. Stylet moderately long, slender, cone straight, shaft cylindrical, with distinct rounded basal knobs, offset from shaft. Pharynx with faintly outlined procorpus and oval-shaped median bulb with distinct valve. Pharyngeal gland lobe variable in length, overlapping intestine ventrally. Hemizonid distinct, at level of excretory pore. Moderately sized tail, gradually tapering to hyaline region, with inflated proctodeum. Phasmids difficult to observe, small, slightly posterior to anus. Hypodermis rounded, marking anterior position of the smooth hyaline region. Tail terminus ending in a broadly rounded tip marked by faint cuticular constrictions.

U.S. Distribution: This species has been reported from San Francisco County, California [14]. After conducting a nematode survey in golf courses from several counties in California, APHIS did not find this nematode, listing this species as not present in the U.S. [15].

Molecular characterization: Subbotin et al. [13] outlined several molecular techniques that have been developed for identification of *M. fallax* including PCR-ITS-RFLP [76], PCR with species-specific SCAR primers [77], size discrimination of IGS PCR products [14,78,96], sequencing of the ITS rRNA [14,97], 18 S rRNA [98], D2-D3 of 28 S rRNA [14,99], *hsp90* [13], *COI* [100], and ITS-based real time TaqMan PCR [101,102] and LAMP assays [79].

Pathogenicity: This species is considered an organism of regulatory importance in U.S. and is listed in the APHIS U.S. Regulated Plant Pest Table [1]. It has a wide host range, which includes several major horticultural and agricultural crops, but was mainly reported on potato. This nematode could lead to total yield losses in potato crops due to quality defects caused to the tubers [12,13]. *M. fallax* is considered a major pest of potato plants and carrots in the Netherlands and on tomatoes in France [16].

Diagnosis: Morphology of *Meloidogyne fallax* is very similar to *M. chitwoodi* from which it differs by having a longer stylet in male and female specimens and by the absence of small irregular outline stylet knobs in both female and male specimens. Additionally, J2 belonging to this species has longer tail and hyaline regions, and different hyaline tail shapes and hemizonid positions when compared to *M. chitwoodi* juveniles. From *M. hapla*, this species can be differentiated by the absence of fine, smooth striae; rounded and flattened dorsal arches; and tail area punctuations in the female perineal pattern and a broader tail and tail terminus with distinct hyaline part in juveniles [97]. Molecularly, *Meloidogyne fallax* can be distinguished from *M. chitwoodi* and other species by the ITS rRNA and *COI* gene sequence [13].

1.9. Litylenchus crenatae Kanzaki et al., 2019 mccannii ssp. Carta, Handoo, Li, Kantor, Bauchan, McCann, Gabriel, Yu, Reed, Koch, Martin, Burke 2020

- *Common name*: North American beech leaf nematode
- *Type plant host*: *Fagus grandifolia*, American beech
- *Type locality*: Perry, OH, U.S.
- *First U.S. report*: 2012, Perry, OH

Measurements: (see Table 6)

Table 6. Morphometrics of *Litylenchus crenatae mccannii* ssp. from Perry, OH. All measurements are given in µm (after Carta et al. [19]).

Character	Adult Female	Young Female	Adult Male
	n = 27	n = 10	n = 4
L	889 ± 119 (625–1084)	823 ± 61 (750–947)	548.0 ± 16.7 (534.5–566.7)
W	14.2 ± 1.0 (12.1–16.1)	11.4 ± 1.1 (9.9–13.5)	15.1 ± 2.5 (12.1–16.7)
Stylet	9.2 ± 0.5 (8.4–10.3)	9.7 ± 0.9 (8.5–11.2)	11.1 ± 0.5 (10.5–11.4)
Stylet conus	4.6 ± 0.4 (3.6–5.2)	-	-
Pharynx	193.5 ± 35.7 (126–244)	152.6 ± 16.2 (133–186)	113.9 ± 5.0 (108.5–118.1)
PUS	34.3 ± 6.1 (22.7–45.0)	-	-
Tail	54.3 ± 6.1 (39.8–64.4)	48.3 ± 6.2 (34.5–56.4)	35.3 ± 1.6 (33.7–37.9)
a	63.0 ± 10.0 (43.8–76.8)	72.9 ± 9.3 (61–86	36.1 ± 5.4 (33.3–44.1)
b	4.7 ± 0.7 (3.8–6.6)	5.4 ± 0.7 (4.5–6.6	4.8 ± 0.2 (4.6–4.9)
c	16.4 ± 1.5 (13.3–20.1)	17.4 ± 3.3 (13–25)	15.5 ± 0.2 (15.3–15.9)
c′	5.7 ± 0.8 (4.3–7.9)	6.0 ± 1.0 (4.3–7.9)	-
V%	76.6 ± 1.4 (73–79)	76.9 ± 1.2 (75–79)	-
PUS/VAD%	27 ± 8 (22–50)	-	-
PUS/BW	2.8 ± 0.5 (1.9–3.8)	-	-
Spicule length	-	-	16.3 ± 1.4 (14.9–17.6)
Gubernaculum	-	-	5.3 ± 0.8 (4.3–6.1)

Description (modified after Carta et al. [19] and Handoo et al. [20]).

Female: Females have a nearly continuous, slightly offset lip region with five annules, long and slender to semi-obese body shape. The stylet is 5% of the pharynx length; median bulb is small, narrow without an obvious valve. The vulval region is kinked and irregular. The anterior gonad is relatively long, almost five times the length of the post uterine sac. The post uterine sac length is about three times the vulval body width and one quarter of the vulval anal distance (VAD). The VAD is 2.8 ± 0.3 (2.3–3.3) µm times the tail length. The rectum is approximately one quarter of the tail length, and the anus is pore-like and obscure in most specimens. There is a gradually tapering, slender, conical tail with an asymmetrically pointed, often mucronate extension. The distal tail in immature and mature females vary in shape.

Male: Males of *Litylenchus crenatae mccannii* ssp. are very similar to *Litylenchus crenatae* males described from Japan. Nematodes have a cylindrical body and assume a smoothly ventrally arcuate shape when killed by gentle heat. Truncate shapes lip region, slightly offset from the body. The stylet is approximately 7–10% of the pharynx length. Lateral field marked by six to eight lines at mid-body.

U.S. Distribution (see Figure 9).

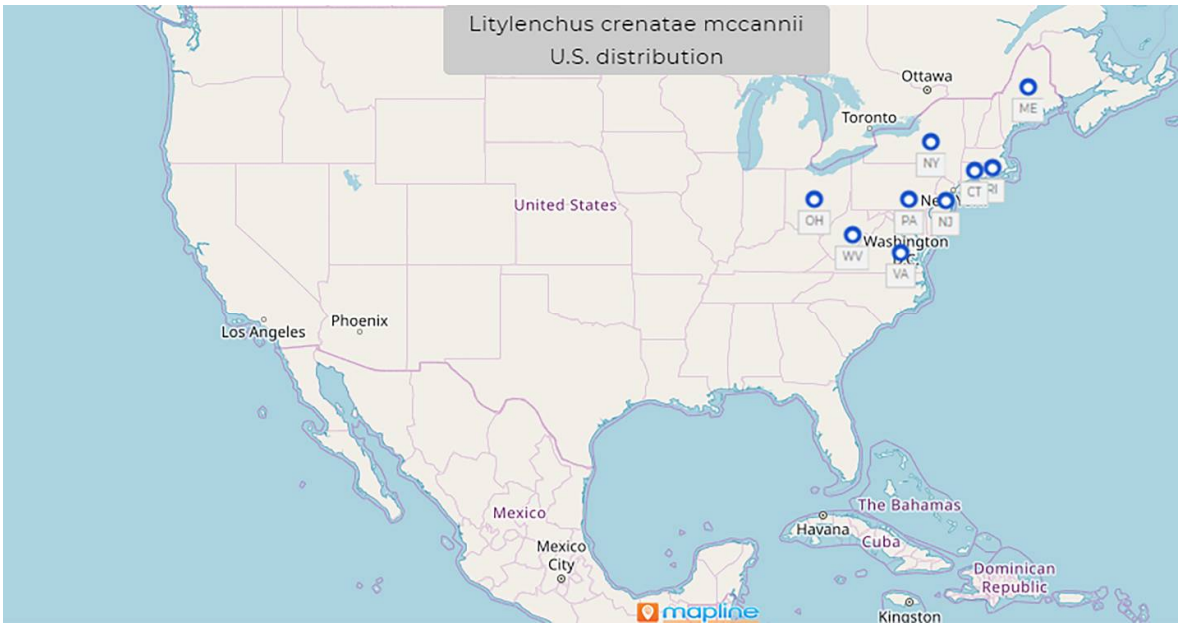

Figure 9. Continental U.S. distribution map of *Litylenchus crenatae mccannii* ssp.

Molecular characterization: Ribosomal DNA marker sequences of *Litylenchus crenatae mccannii* ssp. were nearly identical to the population of *Litylenchus crenatae* from Japan [19]. The internal transcribed spacer (ITS) rDNA and 18 S rDNA sequences for *Litylenchus crenatae* from Japan are 99.7% and 99.9% similar, respectively, to *Litylenchus crenatae mccannii* from North America.

Pathogenicity: Since first reported in U.S. in 2012, this nematode species spread very rapidly through several states in the Northeast U.S., and the latest report of this species from 2021 is approximately 300 miles south from the earliest report from WV [21]. High levels of infection with this nematode in overstory beech trees have been observed. The mortality of infected understory beech trees has been reported after several years of disease [103,104]. This species is not yet a regulated pest in the U.S. However, it is considered an emerging and a highly virulent species that could cause great problems to North American forest ecosystems.

Diagnosis: Morphologically and molecularly, the closest species is *Litylenchus crenatae*. However, young females of *Litylenchus crenatae mccannii* ssp. population can be differentiated from the *Litylenchus crenatae* by having (i) longer stylets 9.7 ± 0.9 (8.6–11.2) vs. 8.0 ± 0.4 (7.4–8.5) µm; (ii) longer stylet conus 4.6 (3.6–5.2) vs. 3.1 (2.8–3.5) µm; and (iii) shorter pharynx (152.6 ± 16.2 vs. 203 ± 5.9 µm). In mature females, a shorter post- uterine sac (36.9 ± 9.4 vs. 68 ± 7.4 µm) was noted in the *Litylenchus crenatae mccannii* specimens. Shorter tail in the fixed immature female populations (48.3 ± 6.2 vs. 55 ± 3.8 µm) but longer in the mature populations (43.7 ± 11.3 vs. 33 ± 2.3 µm). This caused differences in the c (16.8 ± 1.4 vs. 24.5 ± 1.9) and c′ (5.3 ± 1.2 vs. 2.9 ± 0.3) ratios. Narrower body width in mature females in all populations (16.2 ± 2.4 vs. 22.9 ± 2.6 µm) were noted. Some differences between the male specimens from North America and the Japan populations were recorded: (i) longer stylet (11.2 (10.6–12) vs. 10.2 (9.9–11)) µm and stylet conus (4.8 (4.4–5.3) vs. 3.6 (3.5–4.3)) µm; (ii) wider body (16.7 (13.5–20.3)) µm than the fixed type population from Japan [19].

1.10. Pratylenchus fallax Seinforst, 1968

- *Common name*: lesion nematode
- *Type plant host*: *Malus* spp., apple orchard with grass
- *Type locality*: Doornenburg, Netherlands
- *First U.S. report*: 1977, ND

Measurements (see Table 7).

Table 7. Morphometrics of Pratylenchus fallax Seinforst, 1968. All measurements are given in µm.

Character	After Seinhorst [105]		After Saikai et al. [23]	
	Female n = 10	Male n = 10	Female n = 25	Male n = 25
L	420–560	400–500	529 (438–615)	454 (381–543)
W	-	-	20.1 (15.3–23.6)	-
a	23–33	26–33	26.4 (24.1–30.1)	-
b	5.2–6.7	5.0–6.2	54. (4.3–7.5)	-
c	18–24	16–25	21.6 (16.3–28.3)	-
V%	77–81	-	79 (77–81)	-
Postuterine sac	-	-	15.0 (10.6–20.0)	-
Stylet length	16–17	15	15 (13.8–16.4)	13.4 (11.8–14.8)
Tail length	-	-	29 (23.5–36.7)	-
Tail annules	-	-	23 (20–30)	-
Spicule length	-	14–16	-	16.6 (14.0–19.7)
Gubernaculum	-	-	-	4.2 (3.2–6.2)

Description (modified after Saikai et al. [23]).

Female: Body vermiform, straight or slightly curved in specimens killed by gentle heat. Head region with 2–3 annules obscure in most specimens. Posterior edges of cephalic

framework projecting two body annules into body. Stylet knobs anteriorly flattened or pointing forward. Excretory pore at, or posterior to, the level of the nerve ring. Four lines in the lateral field. Usually, there are some additional lines running obliquely between the inner incisures of the lateral field. Ovary outstretched, oocytes in single file except for short region near anterior end of ovary. Spermatheca round, sometimes empty and then narrower and longer than when filled with sperm. Distance between spermatheca and vulva from 42% to 71% of that between vulva and anus. Post vulvar branch about one-fourth to one-third of the vulva–anus distance, its posterior part often consisting of two or three rudimentary elements. Tail conical, with 16–26 narrow annules. Tail tip rounded or with slightly irregular contour, distinctly crenate (generally) to almost smooth (rarely). However, this is only clearly visible in lateral views of tail. In dorsoventral positions (which are the more common in mounted specimens), the annulation is only detected by carefully focusing on the successive incisures. Phasmids at the 9th to 13th annules from tip.

Male: Testis with double row of spermatocytes. Spicules slender, with well-marked manubria and ventrally arcuate shaft. Gubernaculum about 4 µm long; bursa margins distinctly crenate.

U.S. Distribution: This nematode has a limited distribution in U.S., and it has been reported only from North Dakota and more recently (2019) from Wisconsin.

Molecular characterization: Molecular characterization of this species based on 18 S rDNA, the D2–D3 expansion region of 28 S rDNA, and cytochrome c oxidase subunit I (*COI*) as well as by isozymes and ITS-RFLP patterns [23,106–108].

Pathogenicity: *P. fallax* is a regulated pest in the U.S., and luckily, since its first report in the U.S. in 1977, it has been reported only in one more state in 2019. However, recent findings by Bogale et al., 2021 [106], suggest that this species remains a cryptic species among several others in the *P. penetrans* species complex, which could mean that this species could have a wider distribution in the U.S. In Europe, it has a wider distribution, and in the Netherlands, its distribution is especially in sandy or sandy-peat soils in orchards, meadows, and places with natural vegetation [109].

Diagnosis: This species is characterized by having a labial region with two or three often flat and obscure annuli, a conical tail with rounded distinctly crenate tip, a round spermatheca, and rare males (1:5 females). The separation of the two species was confirmed by using different breeding and molecular techniques (isozymes and PCR-RFLP) [106]. It is close to *P. convallariae;* however, it differs by its shorter and narrower body length, higher number of tail annuli, and lower male-to-female ratio. From *P. penetrans*, it differs by having fewer males, a longer pharyngeal overlap, and occasional populations with crenate tails. From *P. pratensis*, it can be distinguished by the rounded spermatheca [109].

2. Conclusions and Future Prospects

Plant-parasitic nematodes are very important pests that can cause significant damage to economically important crops worldwide. This review focused on some quarantine, regulated, and emerging nematode pests reported on the continental U.S., which include *B. xylophillus, D. dipsaci, G. pallida, G. rostochiensis, H. glycines, M. chitwodi, M. enterolobii, M. fallax, L. crenatae mccannii* ssp., and *P. fallax.* The diligence and prompt measures taken by APHIS, the regulatory branch within the U.S. Department of Agriculture, to contain the spread of important quarantine nematodes such as *G. pallida* and *G. rostochiensis* resulted in positive outcomes. Sometimes, the presence of PPNs goes unnoticed in the fields because of a lack of aboveground symptoms of damage, and yield loss may not appear. If undetected and left unmanaged, the nematode population increases rapidly, and it is difficult to reduce population densities once they have reached highly damaging levels, as reported in *H. glycines* [9]. The great magnitude of yield loss caused by *H. glycines* is associated with its widespread distribution, its effective long-term survival in the absence of soybeans, and its ability to consistently reduce yields [9]. If strict measures are not imposed in a timely manner, the spread and distribution of regulated or even emerging plant-parasitic nematodes within U.S. could lead to important economic losses and even

disruption of ecosystems. As it was shown in many cases, continued sampling and scouting for the detection of new infestations of regulated and emerging PPNs are the first and the most important steps toward managing these nematode pests. Early detection of regulated and emerging PPNs is a vital step in preventing the establishment or spread of new nematode pests. Surveys and surveillance should have support from a nematode diagnostic laboratory. Most land grant universities have diagnostic laboratories, but only a few provide nematode diagnostic services that could lead to many important unreported nematode pests. Building a future workforce trained in early identification is equally important. Nematology is a science that needs more attention from federal and state authorities as well as from academia to create career pathways for future generations of nematologists. Prevention is the most cost-effective way to fight pathogens, and it cannot be performed without trained professionals who could prohibit introductions of a nematode's host plant where there is a high risk of transmission. The most important measures for preventing new invasive nematode introductions are restrictions and rigorous control of soil imports, planting materials, growing media, and packing and wood construction materials.

Author Contributions: Conceptualization, M.K. and Z.H.; methodology, Z.H., M.K. and L.C.; software, Z.H., M.K., C.K. and L.C.; validation, Z.H., M.K., C.K. and L.C.; formal analysis, Z.H. and M.K.; investigation, M.K. and Z.H.; resources, Z.H. and M.K.; data curation, Z.H., M.K., C.K. and L.C.; writing original draft preparation, M.K.; writing, review and editing, Z.H., M.K., C.K. and L.C.; visualization, Z.H., M.K., C.K. and L.C.; supervision, Z.H.; project administration, Z.H.; funding acquisition, Z.H. All authors have read and agreed to the published version of the manuscript.

Funding: This research received no external funding.

Institutional Review Board Statement: Not applicable.

Informed Consent Statement: Not applicable.

Data Availability Statement: Not applicable.

Acknowledgments: Mihail Kantor was supported in part by an appointment to the Research Participation Program at the Mycology and Nematology Genetic Diversity and Biology Laboratory USDA, ARS, Northeast Area, Beltsville, MD, administered by the Oak Ridge Institute for Science and Education through an interagency agreement between the U.S. Department of Energy and USDA-ARS. Mention of trade names or commercial products in this publication is solely for the purpose of providing specific information and does not imply recommendation or endorsement by the U.S. Department of Agriculture. USDA is an equal opportunity provider and employer.

Conflicts of Interest: The authors declare no conflict of interest.

References

1. Animal and Plant Health Inspection Service (APHIS). Available online: https://www.aphis.usda.gov/aphis/ourfocus/planthealth/import-information/rppl/rppl-table (accessed on 30 November 2021).
2. National Invasive Species Information Center. Available online: https://www.invasivespeciesinfo.gov/terrestrial/invertebrates (accessed on 30 November 2021).
3. Golden, A.M.; Ellington, D.M. Redescription of Heterodera rostochiensis (Nematoda: Heteroderidae) with a key and notes on closely related species. *Proc. Helminthol. Soc. Wash.* **1972**, *39*, 64–78.
4. Gamalero, E.; Glick, B.R. The use of plant growth-promoting bacteria to prevent nematode damage to plants. *Biology* **2020**, *9*, 381. [CrossRef] [PubMed]
5. Gartner, U.; Hein, I.; Brown, L.H.; Chen, X.; Mantelin, S.; Sharma, S.K.; Dandurand, L.M.; Kuhl, J.C.; Jones, J.T.; Bryan, G.J.; et al. Resisting potato cyst nematodes with resistance. *Front. Plant Sci.* **2021**, *12*, 483. [CrossRef] [PubMed]
6. Haroon, S.A.; Handoo, Z.; Kantor, M.; Skantar, A.; Hult, M. Molecular and morphological characterization of *Globodera rostochiensis* (Wollenweber, 1923) Skarbilovich, 1959 from Egypt. *Not. Sci. Biol.* **2021**, *13*, 11083. [CrossRef]
7. Turner, S.J.; Subbotin, S.A. Cyst Nematodes. In *Plant Nematology*; Perry, R.N., Moens, M., Eds.; CAB International: Wallingford, UK, 2013; pp. 109–143.
8. Animal and Plant Health Inspection Service (APHIS). Available online: https://www.aphis.usda.gov/aphis/ourfocus/planthealth/plant-pest-and-disease-programs/pests-and-diseases/nematode/pcn/ct_pcn_programupdates (accessed on 2 December 2021).

9. Tylka, G.L.; Marett, C.C. Known distribution of the soybean cyst nematode, *Heterodera glycines*, in the United States and Canada in 2020. *Plant Health Progress* **2021**, *22*, 72–74. [CrossRef]
10. Davis, E.L.; Tylka, G.L. Soybean cyst nematode disease. *Plant Health Instr.* **2000**, 1–12. [CrossRef]
11. Ye, W.; Giblin-Davis, R.M. Molecular Characterization and Development of Real-Time PCR Assay for Pine-Wood Nematode *Bursaphelenchus xylophilus* (Nematoda: Parasitaphelenchidae). *PLoS ONE* **2013**, *8*, e78804.
12. European and Mediterranean Plant Protection Organization. PM 3/69 (1) *Meloidogyne chitwoodi* and *M. fallax*: Sampling potato tubers for detection. *Bull. OEPP EPPO Bull.* **2006**, *36*, 421–422. [CrossRef]
13. Subbotin, S.A.; Rius, J.E.P.; Castillo, P. *Systematics of Root-Knot Nematodes (Nematoda: Meloidogynidae)*; Brill: Leiden, The Netherlands, 2021.
14. Nischwitz, C.; Skantar, A.; Handoo, Z.A.; Hult, M.N.; Schmitt, M.E.; McClure, M.A. Occurrence of *Meloidogyne fallax* in North America, and molecular characterization of *M. fallax* and *M. minor* from U.S. golf course greens. *Plant Dis.* **2013**, *97*, 1424–1430. [CrossRef]
15. Anonymous. *Exotic Nematode Survey*; 2012 Final Accomplishment Report; California Department of Food and Agriculture: Sacramento, CA, USA, 2013; p. 7.
16. Haque, Z.; Khan, M.R. *Handbook of Invasive Plant-Parasitic Nematodes: Novel Ingredients for Use in Pet, Aquaculture and Livestock Diets*; Center for Agriculture and Bioscience International: Wallingford, UK, 2021.
17. Castagnone-Sereno, P. *Meloidogyne enterolobii* (= *M. mayaguensis*): Profile of an emerging, highly pathogenic, root-knot nematode species. *Nematology* **2012**, *14*, 133–138. [CrossRef]
18. Brito, J.; Powers, T.O.; Mullin, P.G.; Inserra, R.N.; Dickson, D.W. Morphological and molecular characterization of meloidogyne mayaguensis isolates from Florida. *J. Nematol.* **2004**, *36*, 232. [PubMed]
19. Carta, L.K.; Handoo, Z.A.; Li, S.; Kantor, M.; Bauchan, G.; McCann, D.; Gabriel, C.K.; Yu, Q.; Reed, S.; Koch, J.; et al. Beech leaf disease symptoms caused by newly recognized nematode subspecies *Litylenchus crenatae mccannii* (Anguinata) described from *Fagus grandifolia* in North America. *For. Pathol.* **2020**, *50*, e12580. [CrossRef]
20. Handoo, Z.; Kantor, M.; Carta, L. Taxonomy and Identification of Principal Foliar Nematode Species (Aphelenchoides and Litylenchus). *Plants* **2020**, *9*, 1490. [CrossRef] [PubMed]
21. Kantor, M.R.; Handoo, Z.A.; Carta, L.; Li, S. First report of beech leaf disease, caused by *Litylenchus crenatae* mccannii, on american beech (*Fagus grandifolia*) in Virginia. *Plant Dis.* **2021**, 1–3. [CrossRef] [PubMed]
22. Donald, P.A.; Hosford, R.M., Jr. Plant parasitic nematodes of North Dakota. *Plant Dis.* **1980**, *64*, 45–47. [CrossRef]
23. Saikai, K.; Handoo, Z.A.; MacGuidwin, A.E. First report of the root-Lesion nematode, *Pratylenchus fallax*, on Soybean in Wisconsin, U.S.A. *Plant Dis.* **2019**, *103*, 2141. [CrossRef]
24. Yu, Q.; Potter, J.W.; Gilby, G.A. First report of *Pratylenchus fallax* on turfgrass in Ontario. *Plant Dis.* **1997**, *81*, 1331. [CrossRef]
25. Jeszke, A.; Budziszewska, M.; Dobosz, R.; Stachowiak, A.; Protasewicz, D.; Wieczorek, P.; Obrępalska-Stęplowska, A. A Comparative and Phylogenetic Study of the *Ditylenchus dipsaci*, *Ditylenchus destructor* and *Ditylenchus gigas* Populations Occurring in Poland. *J. Phytopathol.* **2014**, *162*, 61–67. [CrossRef]
26. CABI-ISC. *Invasive Species Compedium*; Center for Agriculture and Bioscience International: Wallingford, UK, 2021; Available online: https://www.cabi.org/isc/datasheet/19287 (accessed on 15 December 2021).
27. Nickle, W.R.; Golden, A.M.; Mamiya, Y.; Wergin, W. On the Taxonomy and Morphology of the Pine Wood Nematode, *Bursaphelenchus xylophilus* (Steiner & Buhrer 1934) Nickle 1970. *J. Nematol.* **1981**, *13*, 385–392.
28. Donald, P.; Stamps, W.T.; Linit, M.J.; Todd, T.C. Pine wilt disease. *Plant Health Instr.* **2003**. [CrossRef]
29. Kikuchi, T.; Aikawa, T.; Oeda, Y.; Karim, N.; Kanzaki, N. A Rapid and Precise Diagnostic Method for Detecting the Pinewood Nematode *Bursaphelenchus xylophilus* by Loop-Mediated Isothermal Amplification. *Phytopathology* **2009**, *99*, 1365–1369. [CrossRef] [PubMed]
30. Thorne, G. *Principles of Nematology*; Mc Graw-Hill: New York, NY, USA, 1961; p. 553.
31. Hooper, D.J. Ditylenchus dipsaci. In *C.I.H. Descriptions of Plant-Parasitic Nematodes*; Set 1:14; Center for Agriculture and Bioscience International: Wallingford, UK, 1972.
32. Mollov, D.S.; Subbotin, S.A.; Rosen, C. First Report of *Ditylenchus dipsaci* on garlic in Minnesota. *Plant Dis.* **2012**, *96*, 1707. [CrossRef] [PubMed]
33. Testen, A.; Walsh, E.K.; Taylor, C.G.; Miller, S.A.; Lopez-Nicora, H.D. First report of bloat nematode (*Ditylenchus dipsaci*) infecting garlic in Ohio. *Plant Dis.* **2014**, *98*, 859. [CrossRef] [PubMed]
34. Loughlin, D. Pests of Ornamental Trees, Shrubs and Flowers. *Int. Pest Control* **2013**, *55*, 220.
35. Sturhan, D.; Brzeski, M.W. Stem and Bulb Nematodes, Ditylenchus spp. In *Manual of Agricultural Nematology*; Nickle, W.R., Ed.; Marcel Dekker: New York, NY, USA, 1991.
36. Subbotin, S.A.; Madani, M.; Krall, E.; Sturhan, D.; Moens, M. Molecular diagnostics, taxonomy, and phylogeny of the stem nematode Ditylenchus dipsaci species complex based on the sequences of the internal transcribed spacer-rDNA. *Phytopathology* **2005**, *95*, 1308–1315. [CrossRef] [PubMed]
37. Andrássy, I. Free-living nematodes of Hungary (Nematoda Errantia) II. In *Pedazoologica Hungarica*; No. 4; Systematic Zoology Research Group of the Hungarian Academy of Sciences: Budapest, Hungary, 2007; p. 496.

38. Vovlas, N.; Troccoli, A.; Palomares-Rius, J.E.; De Luca, F.; Liébanas, G.; Landa, B.B.; Subbotin, S.A.; Castillo, P. Ditylenchus gigas n. sp. parasitizing broad bean: A new stem nematode singled out from the Ditylenchus dipsaci species complex using a polyphasic approach with molecular phylogeny. *Plant Pathol.* **2011**, *60*, 762–775. [CrossRef]
39. Karssen, G.; Willemsen, N.M. The spiculum: An additional useful character for the identification of *Ditylenchus dipsaci* and *D. destructor* (Nematoda: Anguinidae). *EPPO Bull.* **2010**, *40*, 211–212. [CrossRef]
40. Skantar, A.M.; Handoo, Z.A.; Carta, L.K.; Chitwood, D.J. Morphological and molecular identification of globodera pallida associated with potato in Idaho. *J. Nematol.* **2007**, *39*, 133.
41. Subbotin, S.A.; Franco, J.; Knoetze, R.; Roubtsova, T.V.; Bostock, R.M.; Del Prado Vera, I.C. DNA barcoding, phylogeny and phylogeography of the cyst nematode species from the genus Globodera (Tylenchida: Heteroderidae). *Nematology* **2020**, *22*, 269–297. [CrossRef]
42. Camacho, M.J.; Inácio, M.L.; Mota, M.; de Andrade, E. Development and Validation of a Loop-Mediated Isothermal Amplification Diagnostic Method to Detect the Quarantine Potato Pale Cyst Nematode, Globodera pallida. *Pathogens* **2021**, *10*, 744. [CrossRef]
43. Wasala, S.K.; Howe, D.K.; Dandurand, L.M.; Zasada, I.A.; Denver, D.R. Genomic analyses of *Globodera pallida*, a quarantine agricultural pathogen in Idaho. *Pathogens* **2021**, *10*, 363. [CrossRef]
44. Wollenweber, H.W. Krankheiten und Beschadigungen der Kartoffel. *Arb. Forsch. Inst. Kartoff.* **1923**, *7*, 1–56.
45. Manduric, S.; Olsson, E.; Englund, J.-E.; Andersson, S. Separation of *Globodera rostochiensis* and *G. pallida* (Tylenchida: Heteroderidae) using morphology and morphometrics. *Nematology* **2004**, *6*, 171–181. [CrossRef]
46. Stone, A. *Heterodera pallida* N. Sp. (Nematoda: Heteroderidae), a second species of potato cyst nematode. *Nematology* **1972**, *18*, 591–606. [CrossRef]
47. Lownsbery, B.F.; Lownsbery, J.W. *Heterodera tabacurn* new species, a parasite of solanaceous plants in Connecticut. *Proc. Helminthol. Soc. Wash.* **1954**, *21*, 42–47.
48. Miller, L.I.; Gray, B.J. Horsenettle cyst nematode, *Heterodera virginiae* n. sp., a parasite of solanaceous plants. *Nematology* **1968**, *14*, 535–543. [CrossRef]
49. Miller, L.I.; Gray, B.J. *Heterodera solanacearurn* n. sp., a parasite of solanaceous plants. *Nematologica* **1972**, *18*, 404–413. [CrossRef]
50. Golden, A.M.; Klindic, O. *Heterodera achilleae* n. sp. (Nematoda: Heterocleridae) from yarrow in Yugoslavia. *J. Nematol.* **1973**, *5*, 196–201.
51. Brzeski, M.W. *Nematodes of Tylenchina in Poland and Temperate Europe*; Muzeum I lnstytut Zoologii Polska Akademia Nauk: Warsaw, Poland, 1998; p. 396.
52. Eroshenko, A.S.; Kasachenko, I.P. *Heterodera arternisiae* sp. n. (Nematoda: Heteroderidae)-a new cyst-forming nematode species from the Primorsk territory. *Parazitologiya* **1972**, *6*, 166–170. (In Russian)
53. Subbotin, S.A.; Mundo-Ocampo, M.; Baldwin, J.G. *Systematics of Cyst Nematodes (Nematoda: Heteroderinae)*; Part A; Brill: Leiden, The Netherlands, 2010; Volume 8.
54. Cannon, O.S. *Heterodera schachtii* found in a Long Island potato field. *Plant Dis. Rep.* **1941**, *25*, 408.
55. Spears, J.F. The golden nematode handbook. In *Agriculture Handbook No. 353*; U. S. Department of Agriculture: Washington, DC, USA, 1968; pp. 1–81.
56. Animal and Plant Health Inspection Service (APHIS). Available online: https://www.aphis.usda.gov/aphis/ourfocus/planthealth/plant-pest-and-disease-programs/pests-and-diseases/golden-nematode/nematodes (accessed on 23 December 2021).
57. Skantar, A.M.; Handoo, Z.A.; Zasada, I.A.; Ingham, R.E.; Carta, L.K.; Chitwood, D.J. Morphological and Molecular Characterization of Globodera Populations from Oregon and Idaho. *Phytopathology* **2011**, *101*, 480–491. [CrossRef]
58. Wainer, J.; Dinh, Q. Taxonomy, Morphological and Molecular Identification of the Potato Cyst Nematodes, *Globodera pallida* and *G. rostochiensis*. *Plants* **2021**, *10*, 184. [CrossRef]
59. Bulman, S.R.; Marshall, J.W. Differentiation of Australasian potato cyst nematode (PCN) populations using the polymerase chain reaction (PCR). *N. Z. J. Crop Hortic. Sci.* **1997**, *25*, 123–129. [CrossRef]
60. Peng, D.; Shiqi, P.H. Globodera Rostochiensis SCAR Mark as Well as LAMP Fast Detection Method and Application of Method. CN 104059909A, 24 September 2014.
61. Peng, D.; Shiqi, P.H. Globodera rostochiensis SCARMark and LAMPMethod for Quick and Application. CN 104059909B, 4 May 2016.
62. Brodie, B.B.; Mai, W.F. Control of the Golden Nematode in the United States. *Annu. Rev. Phytopathol.* **1989**, *27*, 443–461. [CrossRef]
63. Hirschmann, H. Comparative morphological studies on the soybean cyst nematode, *Heterodera glycines*, and the clover cyst nematode, *H. trifolii* (Nematoda:Heteroderidae). *Proc. Helminthol. Soc. Wash.* **1956**, *23*, 140–151.
64. Burrows, P.R.; Stone, A.R. Heterodera glycines. In *CIH Description of Plant-Parasitic Nematodes*; Set 8 (No. 118); Center for Agriculture and Bioscience International: Wallingford, UK, 1985.
65. Wang, X.; Bergstrom, G.C.; Chen, S.; Thurston, D.M.; Cummings, J.; Handoo, Z.A.; Hult, M.N.; Skantar, A.M. First Report of the Soybean Cyst Nematode, Heterodera glycines, in New York. *Plant Dis.* **2017**, *101*, 1957. [CrossRef]
66. Subbotin, S.A.; Mundo-Ocampo, M.L.; Baldwin, J.G. *Systematics of Cyst Nematodes (Nematoda: Heteroderinae)*; Part B; Brill: Leiden, The Netherlands, 2010.
67. Handoo, Z.A.; Subbotin, S.A. Taxonomy, Identification and Principal Species. In *Cyst Nematodes*; Center for Agriculture and Bioscience International: Wallingford, UK, 2018; pp. 365–398.

68. Ko, H.R.; Kang, H.; Park, E.H.; Kim, E.H.; Lee, J.K. Identification of *Heterodera glycines* (Tylenchida; Heteroderidae) Using qPCR. *Plant Pathol. J.* **2019**, *35*, 654–661. [CrossRef]
69. Allen, T.W.; Bradley, C.A.; Sisson, A.J.; Byamukama, E.; Chilvers, M.I.; Coker, C.M.; Collins, A.A.; Damicone, J.P.; Dorrance, A.E.; Dufault, N.S.; et al. Soybean yield loss estimates due to diseases in the United States and Ontario, Canada, from 2010 to 2014. *Plant Health Prog.* **2017**, *18*, 19–27. [CrossRef]
70. Koenning, S.R.; Wrather, J.A. Suppression of soybean yield potential in the continental United States by plant diseases from 2006 to 2009. *Plant Health Prog.* **2010**, *11*, 11. [CrossRef]
71. Bandara, A.Y.; Weerasooriya, D.K.; Bradley, C.A.; Allen, T.W.; Esker, P.D. Dissecting the economic impact of soybean diseases in the United States over two decades. *PLoS ONE* **2020**, *15*, e0231141.
72. Niblack, T.L.; Colgrove, A.L.; Colgrove, K.; Bond, J.P. Shift in virulence of soybean cyst nematode is associated with use of resistance from PI 88788. *Plant Health Prog.* **2008**, *9*, 29. [CrossRef]
73. Golden, A.M.; O'Bannon, J.H.; Santo, G.S.; Finley, A.M. Description and SEM Observations of *Meloidogyne chitwoodi* n. sp. (Meloidogynidae), a Root-knot Nematode on Potato in the Pacific Northwest. *J. Nematol.* **1980**, *12*, 319.
74. Eisenback, J.D.; Triantaphyllou, H.H. Root-knot Nematodes: Meloidogyne species and races. In *Manual of Agricultural Nematology*; Nickle, W.R., Ed.; Marcel Dekker: New York, NY, USA, 1991.
75. Zijlstra, C.; Lever, A.E.M.; Uenk, B.J.; Van Silfhout, C.H. Differences between ITS regions of isolates of root-knot nematodes *Meloidogyne hapla* and *M. chitwoodi*. *Phytopathology* **1995**, *85*, 1231–1237. [CrossRef]
76. Zijlstra, C.; Uenk, B.J.; Van Silfhout, C.H. A reliable, precise method to differentiate species of root-knot nematodes in mixtures on the basis of ITS-RFLPs. *Fundam. Appl. Nematol.* **1997**, *20*, 59–63.
77. Zijlstra, C.; Donkers-Venne, D.T.; Fargette, M. Identification of Meloidogyne incognita, *M. javanica* and *M. arenaria* using sequence characterised amplified region (SCAR) based PCR assays. *Nematology* **2000**, *2*, 847–853.
78. Wishart, J.; Phillips, M.S.; Blok, V.C. Ribosomal Intergenic Spacer: A Polymerase Chain Reaction Diagnostic for *Meloidogyne chitwoodi*, *M. fallax*, and *M. hapla*. *Phytopathology* **2002**, *92*, 884–892. [CrossRef]
79. Zhang, L.; Gleason, C. Loop-Mediated Isothermal Amplification for the Diagnostic Detection of Meloidogyne chitwoodi and *M. fallax*. *Plant Dis.* **2019**, *103*, 12–18. [CrossRef] [PubMed]
80. Ingham, R.E.; Hamm, P.B.; Ocamb, C.M. Potato (*Solanum tuberosum*)–Nematode, Root-Knot. In *Pacific Northwest Plant Disease Management Handbook*; Oregon State University: Corvallis, OR, USA, 2018.
81. FINDMe.org. Available online: https://www.findmenematode.org/about-findme (accessed on 28 December 2021).
82. Blok, V.C.; Phillips, M.S.; Fargette, M. Comparison of Sequences from the Ribosomal DNA Intergenic Region of Meloidogyne mayaguensis and Other Major Tropical Root-Knot Nematodes. *J. Nematol.* **1997**, *29*, 16.
83. Blok, V.C.; Wishart, J.; Fargette, M.; Phillips, M. Mitochondrial DNA differences distinguishing *Meloidogyne mayaguensis* from the major species of tropical root-knot nematodes. *Nematology* **2002**, *4*, 773–781. [CrossRef]
84. Xu, J.; Liu, P.; Meng, Q.; Long, H. Characterisation of Meloidogyne species from China using Isozyme Phenotypes and Amplified Mitochondrial DNA Restriction Fragment Length Polymorphism. *Eur. J. Plant Pathol.* **2004**, *110*, 309–315. [CrossRef]
85. Kiewnick, S.; Holterman, M.; van den Elsen, S.; van Megen, H.; Frey, J.E.; Helder, J. Comparison of two short DNA barcoding loci (COI and COII) and two longer ribosomal DNA genes (SSU & LSU rRNA) for specimen identification among quarantine root-knot nematodes (*Meloidogyne* spp.) and their close relatives. *Eur. J. Plant Pathol.* **2014**, *140*, 97–110.
86. Long, H.; Wang, X.; Xu, J. Molecular cloning and life-stage expression pattern of a new chorismate mutase gene from the root-Knot nematode Meloidogyne arenaria. *Plant Pathol.* **2006**, *55*, 559–563. [CrossRef]
87. Tigano, M.; De Siqueira, K.; Castagnone-Sereno, P.; Mulet, K.; Queiroz, P.; Dos Santos, M.; Teixeira, C.; Almeida, M.; Silva, J.; Carneiro, R.M.D.G. Genetic diversity of the root-knot nematode Meloidogyne enterolobii and development of a SCAR marker for this guava-damaging species. *Plant Pathol.* **2010**, *59*, 1054–1061. [CrossRef]
88. Niu, J.H.; Jian, H.; Guo, Q.X.; Chen, C.L.; Wang, X.Y.; Liu, Q.; Guo, Y.D. Evaluation of loop-mediated isothermal amplification (LAMP) assays based on 5S rDNA-IGS2 regions for detecting Meloidogyne enterolobii. *Plant Pathol.* **2012**, *61*, 809–819. [CrossRef]
89. He, X.F.; Peng, H.; Ding, Z.; He, W.T.; Huang, W.K.; Peng, D.L. Loop-mediated isothermal amplification assay for rapid diagnosis of Meloidogyne enterolobii directly from infected plants. *Sci. Agric. Sin.* **2013**, *46*, 534–544.
90. Kiewnick, S.; Frey, J.E.; Braun-Kiewnick, A. Development and Validation of LNA-Based Quantitative Real-Time PCR Assays for Detection and Identification of the Root-Knot Nematode Meloidogyne enterolobii in Complex DNA Backgrounds. *Phytopathology.* **2015**, *105*, 1245–1249. [CrossRef]
91. Braun-Kiewnick, A.; Viaene, N.; Folcher, L.; Ollivier, F.; Anthoine, G.; Niere, B.; Sapp, M.; van de Vossenberg, B.; Toktay, H.; Kiewnick, S. Assessment of a new qPCR tool for the detection and identification of the root-knot nematode Meloidogyne enterolobii by an international test performance study. *Eur. J. Plant Pathol.* **2016**, *144*, 97–108. [CrossRef]
92. Subbotin, S.A. Recombinase polymerase amplification assay for rapid detection of the root-knot nematode Meloidogyne enterolobii. *Nematology* **2019**, *21*, 243–251. [CrossRef]
93. Philbrick, A.N.; Adhikari, T.B.; Louws, F.J.; Gorny, A.M. *Meloidogyne enterolobii*, a Major Threat to Tomato Production: Current Status and Future Prospects for Its Management. *Front. Plant Sci.* **2020**, *11*, 1773. [CrossRef]
94. Hunt, D.J.; Handoo, Z.A. Taxonomy, identification and principal species. In *Root-Knot Nematodes*; Center for Agriculture and Bioscience International: Wallingford, UK, 2009; Volume 1, pp. 55–97.

95. Karssen, G. Description of *Meloidogyne fallax* n. sp. (Nematoda: Heteroderidae), a root-knot nematode from The Netherlands. *Fundam. Appl. Nematol.* **1996**, *19*, 593–600.
96. Holterman, M.H.; Oggenfuss, M.; Frey, J.E.; Kiewnick, S. Evaluation of High-resolution Melting Curve Analysis as a New Tool for Root-knot Nematode Diagnostics. *J. Phytopathol.* **2012**, *160*, 59–66. [CrossRef]
97. Karssen, G.; Bolk, R.J.; Van Aelst, A.; van den Beld, I.; Kox, L.; Korthals, G.; Molendijk, L.; Zijlstra, C.; Van Hoof, R.; Cook, R. Description of *Meloidogyne minor* n. sp. (Nematoda: Meloidogynidae), a root-knot nematode associated with yellow patch disease in golf courses. *Nematology* **2004**, *6*, 59–72. [CrossRef]
98. Holterman, M.; Karssen, G.; van den Elsen, S.; Van Megen, H.; Bakker, J.; Helder, J. Small subunit rDNA-based phylogeny of the Tylenchida sheds light on relationships among some high-impact plant-parasitic nematodes and the evolution of plant feeding. *Phytopathology* **2009**, *99*, 227–235. [CrossRef] [PubMed]
99. Shah, F.A.; Falloon, R.E.; Bulman, S.R. Nightshade weeds (*Solanum* spp.) confirmed as hosts of the potato pathogens *Meloidogyne fallax* and *Spongospora subterranea* f. sp. subterranea. *Australas. Plant Pathol.* **2010**, *39*, 492–498. [CrossRef]
100. Hodgetts, J.; Ostojá-Starzewski, J.C.; Prior, T.; Lawson, R.; Hall, J.; Boonham, N. DNA barcoding for biosecurity: Case studies from the UK plant protection program. *Genome* **2016**, *59*, 1033–1048. [CrossRef] [PubMed]
101. Zijlstra, C.; Van Hoof, R.A. A Multiplex Real-Time Polymerase Chain Reaction (TaqMan) Assay for the Simultaneous Detection of Meloidogyne chitwoodi and M. fallax. *Phytopathology* **2006**, *96*, 1255–1262. [CrossRef]
102. De Haan, E.G.; Dekker, C.C.E.M.; Tameling, W.I.L.; den Nijs, L.J.M.F.D.; van den Bovenkamp, G.W.; Kooman-Gersmann, M. The MeloTuber Test: A real-time TaqMan® PCR-based assay to detect the root-knot nematodes Meloidogyne chitwoodi and M. fallax directly in potato tubers. *EPPO Bull.* **2014**, *44*, 166–175. [CrossRef]
103. Reed, S.E.; Greifenhagen, S.; Yu, Q.; Hoke, A.; Burke, D.J.; Carta, L.K.; Handoo, Z.A.; Kantor, M.R.; Koch, J. Foliar nematode, *Litylenchus crenatae* ssp. *mccannii*, population dynamics in leaves and buds of beech leaf disease-affected trees in Canada and the US. *For. Pathol.* **2020**, *50*, e12599. [CrossRef]
104. Ewing, C.J.; Hausman, C.E.; Pogacnik, J.; Slot, J.; Bonello, P. Beech leaf disease: An emerging forest epidemic. *For. Pathol.* **2019**, *49*, 12488. [CrossRef]
105. Seinhorst, J.W. Pratylenchus fallax. In *CIH-Descriptions of Plant-Parasitic Nematodes Set 7*; No. 100; Center for Agriculture and Bioscience International: Slough, UK, 1977.
106. Bogale, M.; Tadesse, B.; Nuaima, R.; Honermeier, B.; Hallmann, J.; DiGennaro, P. Morphometric and Molecular Diversity among Seven European Isolates of *Pratylenchus penetrans*. *Plants* **2021**, *10*, 674. [CrossRef]
107. Ibrahim, S.K.; Perry, R.N.; Webb, R.M. Use of isoenzyme and protein phenotypes to discriminate between six Pratylenchus species from Great Britain. *Ann. Appl. Biol.* **1995**, *126*, 317–327. [CrossRef]
108. Waeyenberge, L.; Viaene, N.; Moens, M. Species-specific duplex PCR for the detection of Pratylenchus penetrans. *Nematology* **2009**, *11*, 847–857. [CrossRef]
109. Castillo, P.; Vovlas, N. *Pratylenchus (Nematoda: Pratylenchidae): Diagnosis, Biology, Pathogenicity and Management*; Brill: Boston, IL, USA, 2007.